Original article

Detailed analysis and follow-up studies of a high-throughput screening for indoleamine 2,3-dioxygenase 1 (IDO1) inhibitors

CrossMark

Ute F. Röhrig [a], Somi Reddy Majjigapu [a, b], Marc Chambon [c], Sylvian Bron [a], Luc Pilotte [d, e], Didier Colau [d, e], Benoît J. Van den Eynde [d, e], Gerardo Turcatti [c], Pierre Vogel [b], Vincent Zoete [a, *], Olivier Michielin [a, f, g, *]

[a] Swiss Institute of Bioinformatics, Molecular Modeling Group, Quartier Sorge — Bâtiment Génopode, CH-1015 Lausanne, Switzerland
[b] Laboratory of Glycochemistry and Asymmetric Synthesis, Ecole Polytechnique Fédérale de Lausanne (EPFL), CH-1015 Lausanne, Switzerland
[c] Biomolecular Screening Facility, Ecole Polytechnique Fédérale de Lausanne (EPFL), CH-1015 Lausanne, Switzerland
[d] de Duve Institute and the Université catholique de Louvain, B-1200 Brussels, Belgium
[e] Ludwig Institute for Cancer Research, B-1200 Brussels, Belgium
[f] Department of Oncology, University of Lausanne and Centre Hospitalier Universitaire Vaudois (CHUV), CH-1011 Lausanne, Switzerland
[g] Ludwig Center for Cancer Research of the University of Lausanne, CH-1015 Lausanne, Switzerland

A R T I C L E   I N F O

A B S T R A C T

Indoleamine 2,3-dioxygenase 1 (IDO1) is a key regulator of immune responses and therefore an important therapeutic target for the treatment of diseases that involve pathological immune escape, such as cancer. Here, we describe a robust and sensitive high-throughput screen (HTS) for IDO1 inhibitors using the Prestwick Chemical Library of 1200 FDA-approved drugs and the Maybridge HitFinder Collection of 14,000 small molecules. Of the 60 hits selected for follow-up studies, 14 displayed IC_{50} values below 20 μM under the secondary assay conditions, and 4 showed an activity in cellular tests. In view of the high attrition rate we used both experimental and computational techniques to identify and to characterize compounds inhibiting IDO1 through unspecific inhibition mechanisms such as chemical reactivity, redox cycling, or aggregation. One specific IDO1 inhibitor scaffold, the imidazole antifungal agents, was chosen for rational structure-based lead optimization, which led to more soluble and smaller compounds with micromolar activity.

1. Introduction

The kynurenine pathway of tryptophan metabolism has been recognized as a central component of both the nervous [1] and the immune system [2—4]. The enzyme indoleamine 2,3-dioxygenase 1 (IDO1, EC 1.13.11.52) catalyzes the initial and rate-limiting step in tryptophan catabolism [5], leading to the depletion of tryptophan and to the production of kynurenine metabolites, both responsible for local immunosuppression [6]. The immunosuppressive function of IDO1 [7,8] and the functionally related enzyme tryptophan 2,3-dioxygenase (TDO) [9,10] is exploited by tumor cells to escape a potentially effective immune response [6]. As high IDO1 expression is associated with poor prognosis in a variety of cancer types [11], it has been selected as a therapeutic target for pharmacological interventions [12,13]. Results from *in vitro* and *in vivo* studies demonstrate indeed that the efficacy of therapeutic vaccination or chemotherapy may be improved by concomitant administration of an IDO1 inhibitor [7,14,15].

Intense efforts to develop potent, selective IDO1 inhibitors are ongoing in academia and in pharmaceutical companies and have yielded different active scaffolds, such as quinones, indoles, hydroxyamidines, triazoles, and indoles [16]. Two compounds have entered clinical trials, the hydroxyamidine INCB024360 developed

by Incyte [15,17,18] (NCT: NCT01604889, NCT01685255, NCT01822691, NCT01961115), and more recently the imidazole NLG919 from New Link Genetics [19]. High-throughput screening (HTS) has become a routine method for the discovery of new inhibitors, but care must be taken to avoid compound-dependent assay interference artifacts [20]. A few screening campaigns for IDO1 inhibitors have been described. A yeast growth restoration assay conducted with 2500 compounds from the NCI Diversity Set and from algal extracts identified one IDO1 inhibitor with a K_i of 1.5 μM [21]. 50,000 compounds of the ChemBridge DiverSet compound library were subject to a yeast-based screening assay [22], validated by a low hit rate (0.2%) and a high confirmation rate (76%). However, no chemical structures were disclosed. Amgen's compound library (245,000 compounds) has been screened in an enzymatic assay against IDO1 [23], yielding a hit rate of 1.4%. The structure of one hit, Amg-1 with an IC_{50} value of 3 μM, was disclosed. Another screen of the NCI Diversity Set with a new fluorescence detection method [24] yielded 35 hits without disclosing their structures. Recently, a library of 352 fragments was screened on IDO1 using differential scanning fluorimetry as detection method [25]. 51 hits were disclosed, and lead optimization concentrated on the hydrazine scaffold, identifying phenylhydrazine as a nanomolar IDO1 inhibitor.

Review of the screening literature on IDO1 reveals that only selected fractions of the results have been published, for example omitting the identification of promiscuous hits, and often concealing the chemical structures of the active scaffolds. While this is understandable in view of the advantage of nondisclosure when developing new therapeutics, it hampers the discovery of new selective IDO1 inhibitors, as manifest by numerous recent publications describing compounds probably acting through an unspecific inhibition mechanism on IDO1. Here, we describe a HTS for IDO1 inhibitors including a detailed analysis of the hits and extensive follow-up studies to distinguish between specific and promiscuous IDO1 inhibitors. We only leave out the description of two active compounds to allow for their potential further development as therapeutic agents.

In an academic screening effort, we screened two chemical libraries against IDO1, the Prestwick Chemical Library (PCL), which is composed of 1200 FDA-approved drugs, and the Maybridge Hit-Finder Collection (MHC) of 14,000 compounds. The structural overlap between the Maybridge HitFinder Collection and previously screened libraries for which data is publicly available (NCI Diversity Set, Chembridge DiverSet) is very low (23 and 77 compounds respectively). Therefore the possibility of discovering new inhibitor scaffolds through our screening is warranted. Although some FDA approved compounds have previously been tested for IDO1 inhibition [26], no systematic screening has been carried out yet. The advantage of screening a library of FDA-approved compounds is the large amount of available information. This is of value not only for the purpose of drug repositioning [27] but also for evaluating probable modes of action. As many of our screening hits turned out to be false positives, we used known criteria for filtering out HTS interference compounds [28–34] as well as different secondary assays for detecting unspecific inhibition. Oxidative proteins are known to be difficult screening targets, because library compounds capable of redox cycling may indirectly inhibit target activity depending on assay conditions [29,35–37]. False positives can also result from phenomena such as aggregation [28,38], covalent reactivity [34], or interference with the optical readout [20]. We used quantum-chemical calculations to investigate the link between the reduction and oxidation potentials of known redox-cycling compounds and their activity on IDO1. Aggregation was controlled in a secondary assay by addition of small amounts of detergent to the incubation medium [39]. Chemically reactive compounds were detected by structural filters, or, in case of strong electrophiles, subject to an enzymatic assay in presence of high concentrations of a nucleophile. Interference with the optical readout was circumvented by using HPLC separation in the secondary assay. Confirmed hit compounds were subject to a cellular test for murine IDO1 inhibition and counter-screened for murine TDO inhibition. One confirmed active scaffold, the imidazole antifungal agents, was chosen for computer-aided structure-based lead optimization, which we have successfully applied to the design of new IDO1 inhibitors before [40,41]. Here, this approach led to more soluble and smaller compounds with micromolar activity.

2. Results and discussion

### 2.1. High throughput screening

The employed HTS protocol was similar to commonly employed enzymatic assay protocols [41]. Briefly, the reaction mixture contained IDO1, the substrate L-tryptophan, the reducing agents ascorbate and methylene blue, and the library compound at a concentration of 10 μM. After incubation for 60 min at room temperature, the enzymatic reaction was stopped by addition of a hydrogen peroxide solution. Some features of the protocol need to be taken into account when interpreting the screening results. Firstly, to obtain a high-throughput detection method of the enzymatic reaction product N-formyl kynurenine (NFK), no HPLC separation was carried out. Instead, the light absorption of the reaction mixtures was measured at a wavelength of 320 nm before and after incubation with IDO1. However, this wavelength is not very specific for NFK. Screening compounds that undergo chemical modifications during incubation or after addition of hydrogen peroxide may also cause absorbance changes in this region. Secondly, the absence of catalase, which is normally added to the incubation medium [42], could facilitate the oxidation of active, ferrous IDO1 to inactive, ferric IDO1. False positives due to these effects were removed during the secondary assay, when kynurenine was quantified after HPLC separation and catalase was added to the incubation medium.

An example of the screening result for one 384-well plate is given in Fig. 1A. The first 32 wells were used for the negative control (no inhibitor present, cyan squares), while the last 32 wells were used for the positive control (reference inhibitor present, green squares). Here, we used our previously developed inhibitor 4-(3-bromophenyl)-1,2,3-triazole [41] (IC_{50} = 2.0 μM) at a concentration of 50 μM as positive reference. At this concentration a complete inhibition of IDO1 activity was achieved, as we previously confirmed by HPLC analysis. A HTS score of zero was assigned to the average absorbance change at 320 nm of the negative control samples, while a score of one was assigned to the average absorbance change of the positive control samples.

The blue shaded area in Fig. 1A denotes the average ±3 standard deviations of the negative control, while the green shaded area denotes the average ±3 standard deviations of the positive control. The calculated Z' value [43] for this plate is 0.80 and demonstrates the excellent reproducibility and sensitivity of the employed screening protocol. The Z' values for each individual screening plate ranged from 0.74 to 0.86. The cumulative interplate Z' was 0.8, illustrating the good quality and robustness of the screening assay. Using a HTS score cutoff of 0.2 to define a hit, 36 hits were obtained for the PCL (3.0%) and 183 hits for the MHC (1.3%).

2.2. Structural and functional analysis of the PCL hits

Based on the large amount of literature available for the FDA-approved compounds of the PCL, we developed the hypothesis
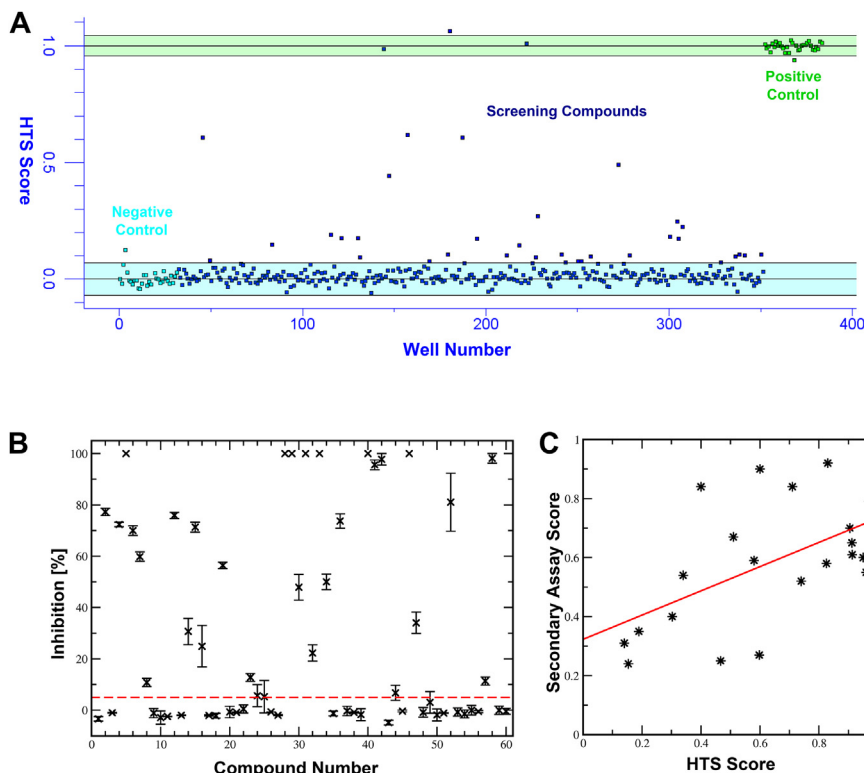
Fig. 1. A. HTS results for one sample plate. Each dark blue spot corresponds to one library compound. B. Results of the single-point assay for the 60 purchased compounds from the PCL and the MHC. Compounds producing less than 5% of inhibition (dashed line) were classified as inactives and are thus false positives of the HTS. C. Correlation between the HTS score and the score of the secondary assay calculated at a concentration of 10 µM for the active compounds (correlation coefficient = 0.55). (For interpretation of the references to color in this figure legend, the reader is referred to the web version of this article.)

that many of the identified hits act through unspecific inhibition on IDO1 for one or more of the following reasons.

- Redox-cycling compounds may interfere with the active reduced state of IDO1 under the HTS assay conditions (e.g. ebselen, primaquine, idebenone, chrysene-1,4-quinone, anthralin, eseroline, nisoldipine, lacidipine, nifedipine, disulfiram) [37].
- Iron chelators may interfere with the heme cofactor (e.g. ciclopirox, disulfiram, deferoxamine, mercaptopurine) [44].
- Tetracycline antibiotics (e.g. lymecycline, oxytetracycline, doxycycline) might act through a redox mechanism or as iron chelators [45]
- Some compounds may inhibit IDO1 through chemical reactivity, for example the alkylating agent dacarbazine.
- Aggregators may promiscuously inhibit enzymes by denaturation (miconazole, econazole, and sulconazole) [28].
- Dye molecules could produce a signal by changing absorption at 320 nm during incubation or after addition of hydrogen peroxide (e.g. Chicago sky blue, propidium iodide, merbromin).

To test our hypotheses, some of these compounds were chosen for experimental follow-up studies. These include miconazole (HTS score 0.91), sulconazole (0.91), econazole (0.83), ciclopirox (0.61), mercaptopurine (0.61), disulfiram (0.59), nisoldipine (0.42), lacidipine (0.22), and nifedipine (0.09). Additionally, 14 compounds were chosen for further testing:

- The imidazole antifungal drugs sertaconazole (score 0.91), tioconazole (0.68), oxiconazole (0.60), isoconazole (0.47),

butoconazole (0.34), enilconazole (0.19), ketoconazole (0.15), and bifonazole (0.14). These are known to inhibit the enzyme CYP51A1 (lanosterol 14 α-demethylase), a heme-containing cytochrome P450 [46] but they could also act unspecifically through aggregation [28].
- Rabeprazole (0.75), a proton pump inhibitor.
- Phenelzine (0.30), an irreversible monoamine oxidase inhibitor of the hydrazine class, which has been suggested to modulate drug metabolism through heme binding in cytochrome P-450 [47].
- Amiodarone (0.21), an antiarrhythmic agent.
- Phentermine (0.15), a psychostimulant drug and appetite suppressant.
- Liranaftate (0.15), a squalene epoxidase inhibitor used as an antifungal.
- Raloxifene (0.14), a selective estrogen receptor modulator.

Our hits show a good overlap with the recently described FDA-approved compounds active on mIDO1 [26], which included some anti-fungal imidazoles (miconazole, econazole, clotrimazole, sulconazole) as well as lansoprazole, fenretinide, nifedipine, and troglitazone.
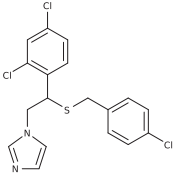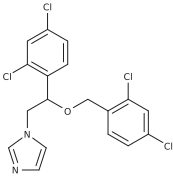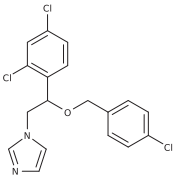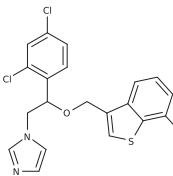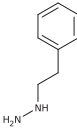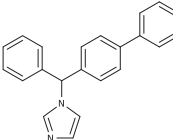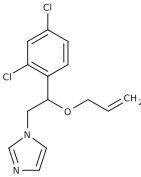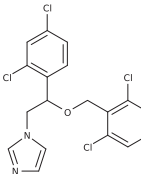
See SI Table S1 for a list of all 23 purchased compounds from the PCL, ranked according to their enzymatic IC_{50} value measured under standard conditions.

2.3. Structural and functional analysis of the MHC hits

The hits from the MHC were also analyzed structurally and functionally. Again, many of these compounds were identified as
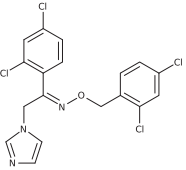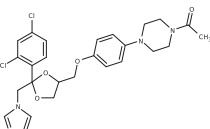
Table 1
Results for all confirmed hits of the Prestwick Chemical Library (PCL). Name, chemical structure, number of failed structural filters (FScore), enzymatic IC_{50} value on hIDO under standard conditions and with 0.01% Triton-X added, cellular IC_{50} value on mIDO, cellular IC_{50} value on mTDO, cellular LD_{50} value. All values are given in μM. NI: no inhibition. ND: not determined.

Name	Structure	FScore	Enzymatic tests		Cellular tests		
			IC_{50}/standard	IC_{50}/Triton	IC_{50}/mIDO	IC_{50}/mTDO	LD_{50}
Sulconazole		0	6.4	ND	NI	NI	10
Miconazole		1	6.7	3.8	NI	NI	10
Econazole		0	8.1	ND	NI	NI	10
Sertaconazole		0	8.4	ND	NI	NI	10
Phenelzine		1	14	ND	NI	NI	>25
Bifonazole		0	23	ND	NI	NI	10
Enilconazole		1	23	ND	NI	NI	>25
Isoconazole		1	23	ND	NI	NI	10

(*continued on next page*)

Table 1 (*continued*)

Name	Structure	FScore	Enzymatic tests		Cellular tests		
			IC$_{50}$/standard	IC$_{50}$/Triton	IC$_{50}$/mIDO	IC$_{50}$/mTDO	LD$_{50}$
Oxiconazole		1	28	ND	NI	NI	10
Ketoconazole		2	32	25	NI	NI	25

potential unspecific inhibitors because of redox-cycling capacities, chemical reactivity, iron chelation, or strong optical absorption.

It is noteworthy that the five top-ranking hits from the MHC were all *para*-quinones, which were also strongly enriched among the screening hits (0.2% of the MHC, 5.5% of the hits). A similar enrichment was observed for thiosemicarbazones, known iron chelators (0.7% of the MHC, 13.7% of the hits).

We clustered compounds according to common chemical motifs, and one or a few representatives of each group were chosen for follow-up studies. A total of 37 compounds was acquired, ranging from 0.97 to 0.21 in the screening score (SI Table S2).

2.4. Experimental follow-up studies

2.4.1. In vitro assay

For detailed single-point and dose–response studies, we quantified kynurenine production and tryptophan degradation precisely by HPLC. Chromatographic separation of the reaction mixture into its components allows for the use of higher amounts of the reductive co-factors (ascorbate and methylene blue) as well as the presence of catalase, shown to be necessary for the removal of hydrogen peroxide from the medium [42]. Additionally, chromatographic separation prevents the interference of colored compounds with the detection of the enzymatic reaction product.

2.4.2. Single-point activities at highest soluble concentration

In order to be able to detect even weak IDO1 inhibitory activity among the 60 purchased compounds, we tested each compound at its previously determined highest soluble concentration (in phosphate buffer at pH 6.5 containing 5% DMSO). The results are given in Fig. 1B, SI Tables S1 and S2. About half of the compounds (31 compounds, 52%) displayed more than 5% of IDO1 inhibitory activity in this test, while the other half were inactive and therefore false positives of the HTS. The HTS score does not allow filtering out the false positives as they show scores in a wide range between 0.84 and 0.09.

From the PCL, only phenelzine and most of the imidazole antifungal agents were confirmed as positives. As expected, the false positives included the compounds ciclopirox, disulfiram, mercaptopurine, nisoldipine, lacidipine, and nifedipine. However, also the imidazole antifungal agents butoconazole and tioconazole as well as the drugs amiodarone, rabeprazole, phentermine, liranaftate, and raloxifene were not confirmed as hits.

From the MHC, 17 compounds were selected for IC$_{50}$ determination based on their activity in the single-point assay. The unconfirmed hits included all five tested thiosemicarbazones.

2.4.3. Enzymatic IC$_{50}$ determination

Enzymatic IC$_{50}$ values were determined for the positives from the single-point measurements. The assay conditions were the same as for the single point measurements, except for the concentration of the tested chemical compounds, that was seven times 3-fold diluted from its highest soluble concentration. For 21 compounds an IC$_{50}$ value could be determined, and for 14 compounds this value was below 20 μM (Tables 1 and 2). For the active compounds, a positive correlation was found between the HTS score and the score in the secondary assay calculated at a compound concentration of 10 μM (Fig. 1C, $r = 0.55$), corroborating the validity of the screening protocol for confirmed positives. However, reproduction of measured IC$_{50}$ values in independent experiments was in general more challenging than in case of our previously established inhibitor scaffolds [41], suggesting that they were influenced by an experimental parameter that was not systematically monitored.
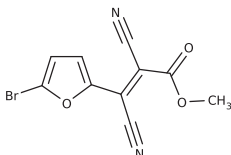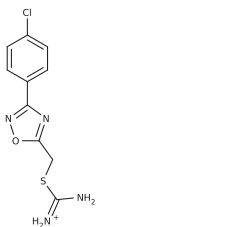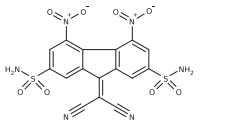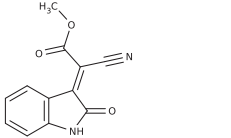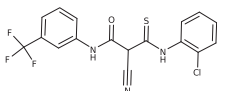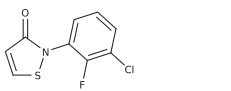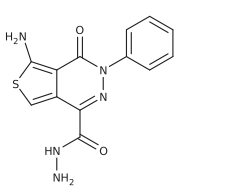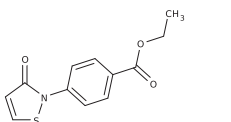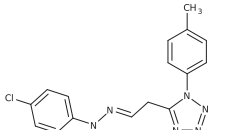
From the PCL, nine imidazole antifungal agents showed a micromolar IC$_{50}$ value (Table 1). The only structurally distinct hit from the PCL was phenelzine (phenylethylhydrazine) with an IC$_{50}$ value of 12 μM. It is known that hydrazine can directly bind to the ferrous heme of cytochrome P450 (CYP) [47], so an interaction with the active site heme of IDO1 is probable. Indeed, our docking results suggest that the hydrazine group can bind to the heme iron of IDO1, locating the phenyl ring in the buried hydrophobic A pocket (Fig. 2A). This binding mode is in agreement with the recently proposed binding mode of phenylhydrazine (IC$_{50}$ = 0.25 μM) [25].

For eleven compounds from the MHC, an IC$_{50}$ value could be determined. The structures and results for these compounds, except for two undisclosed compounds, are shown in Table 2.

2.4.4. Cellular IC$_{50}$ and LD$_{50}$ determination

We tested compounds with a low IC$_{50}$ in the enzymatic assay for their ability to inhibit tryptophan degradation and kynurenine production in cells expressing murine (mIDO1). Murine IDO1 shares 62% of sequence identity with human IDO1 [48], and the active site residues are 100% conserved. In an earlier work we found an excellent correlation between cellular assay results on mIDO1 and on hIDO1 ($r = 0.95$) [41]. Such cellular assay is informative for drug development, as it evaluates not only the IDO1 inhibitory

Table 2

Results for the confirmed hits from the Maybridge HitFinder Collection (MHC), excluding two undisclosed compounds. Product code, chemical structure, number of failed structural filters (FScore), enzymatic IC_{50} values on hIDO under standard conditions and with 5 mM GSH or 0.01% Triton-X added, cellular IC_{50} value on mIDO, cellular IC_{50} value on mTDO, cellular LD_{50} value. All values are given in μM. NI: no inhibition. ND: not determined.

Code	Structure	FScore	Enzymatic tests			Cellular tests		
			IC_{50}/standard	IC_{50}/GSH	IC_{50}/Triton	IC_{50}/mIDO	IC_{50}/mTDO	LD_{50}
NRB00511		2	0.71	7.1	ND	NI	NI	5
CD02761		3	0.89	ND	1.2	2.1	NI	10
BTB13360		3	1.0	1.6	0.96	NI	NI	>25
S14435		1	1.8	130	ND	NI	NI	>25
DP00477		2	7.0	71	6.3	NI	NI	>25
KM04550		1	11	200	4.8	NI	NI	10
HTS01525		4	13	ND	15	NI	NI	>25
KM04416		1	15	100	11	NI	NI	10
NRB04258		2	54	31	53	0.34	4.2	10
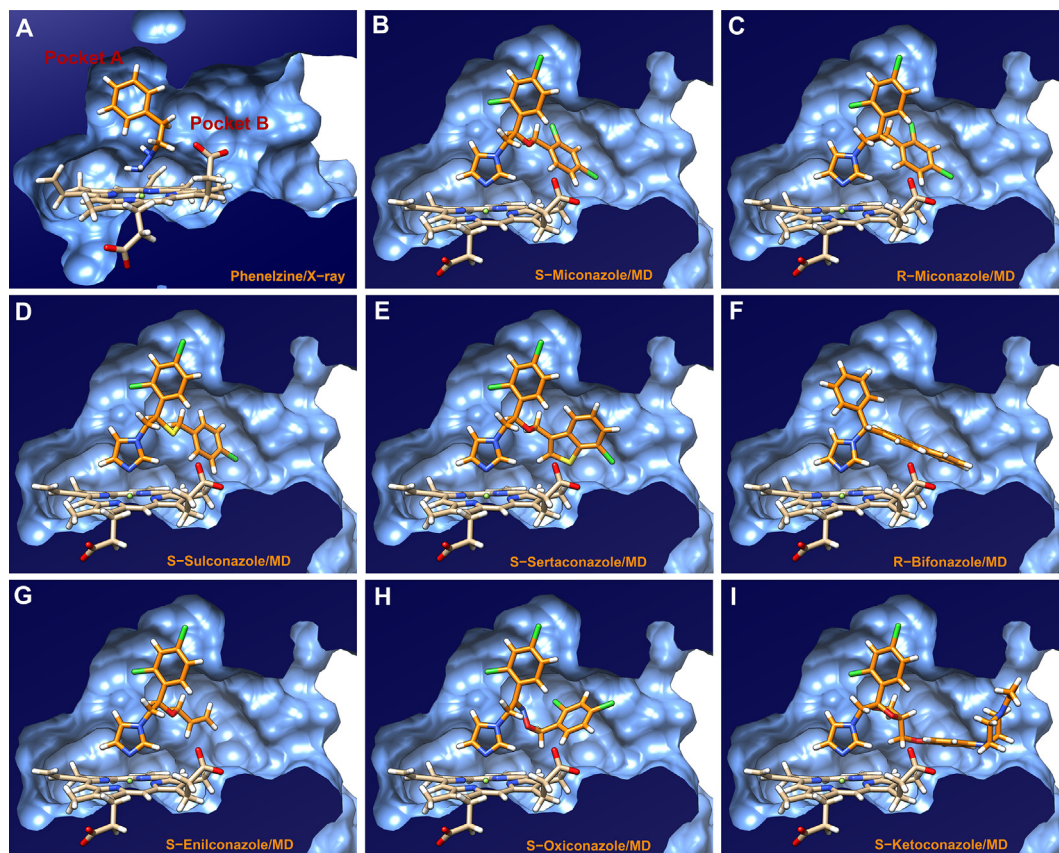
Fig. 2. A. Phenelzine docked into the IDO1 X-ray structure. B–I. Imidazole antifungal agents docked into the IDO1 active site as present after molecular dynamics simulations. As exemplified for miconazole (B, C), both the S and the R enantiomers can be accommodated in the active site.

effect of the compounds but also their capacity to permeate the cell, their inhibition of tryptophan and kynurenine transport, and their potential cytotoxicity. To control specificity, we also tested the inhibitory activity of the compounds on cells expressing murine TDO (mTDO). The same murine cell type, stably transfected with murine IDO1 or TDO, was used for inhibition and cell viability assays.

Inhibition tests on mIDO1 and mTDO at a maximal concentration of 25 μM yielded negative results for all PCL compounds (Table 1). One reason could be their high toxicity displayed in these tests, resulting in LD_{50} values around 10 μM, except for phenelzine and enilconazole. The observed toxicities for miconazole, econazole, and sulconazole are slightly higher than the ones reported earlier [26], which could be due to the different cell types (P815B here vs. HEK), the different cell quantities (2×10^5 cells here vs. 1×10^5 cells), and the different medium (IMDM-2% FCS here vs. Opti-MEM). In this earlier report, cellular IC_{50} values for these compounds were determined to be 18 μM for miconazole, 11 μM for econazole, and 30 μM for sulconazole [26].

Of the eleven confirmed hits of the MHC, only four showed a LD_{50} value above 25 μM in the cellular assays (Table 2), but these were inactive both on mIDO1 and on mTDO. Four of the remaining compounds showed an activity on mIDO1. By addressing affinity, selectivity, and safety, these active compounds might be pursued for lead optimization.

In summary, the attrition rate among the compounds acquired for follow-up studies of the HTS was very high. Of the 60 acquired compounds, 29 failed the single-point activity assay. For 21 compounds an enzymatic IC_{50} value was obtained, but only for 4

compounds a cellular IC_{50} value could be determined. In order to better understand the effects leading to these results, we investigated some of their potential causes.

2.5. Analysis of unconfirmed or promiscuous hits

2.5.1. Structural filters

Several structural filters for the detection of problematic screening compounds have been developed [30–34], and algorithms for automated filtering are publicly available. The purpose of the Glaxo filter [30] is to describe reactive functional groups, unsuitable leads, and unsuitable natural products. The Pfizer LINT

Table 3
Number of compounds from the screening libraries, the screening hits, and the confirmed hits failing different structural filters for the detection of problematic screening compounds. The total number of compounds for each column is given on top.

Filter	Library		Hits		Confirmed hits	
	PCL	MHC	PCL	MHC	PCL	MHC
			Nr. of Compounds			
	1200	14,000	36	183	10	11
Lilly [34]	423 (35%)	5640 (40%)	20 (56%)	131 (72%)	1 (10%)	10 (91%)
Pfizer LINT [31]	518 (43%)	5850 (42%)	21 (58%)	95 (52%)	5 (50%)	6 (55%)
Abbot ALARM [32]	170 (14%)	2265 (16%)	14 (39%)	75 (41%)	0 (0%)	4 (36%)
Glaxo [30]	134 (11%)	1200 (9%)	5 (14%)	22 (12%)	0 (0%)	1 (9%)
PAINS [33]	21 (2%)	365 (3%)	2 (6%)	10 (5%)	1 (10%)	1 (9%)

filter [31] aims to detect reactive functional groups as well as mutagenic or carcinogenic functionalities. The ALARM filter from Abbott Laboratories is based on a specifically developed NMR assay and predicts thiol reactivity of small molecules [32]. This is of special interest for IDO1, as cystein modification has been shown to inhibit enzymatic activity [49]. The "pan assay interference compounds" (PAINS) filter relies on the analysis of large numbers of screening hits and on literature data mining [33]. Most recently, also Lilly Research Laboratories published an extensive list of rules for identifying reactive or promiscuous compounds based on review by a panel of experienced medicinal chemists [34].

As Table 3 shows, the Lilly Medchem Rules and the Pfizer LINT filters flag the largest numbers of compounds, about 40% of the two screening libraries, while the other filters are more permissive. The failure rates of all filters increase significantly among the screening hits as compared to the full libraries, indicating that the hits contain a higher number of problematic compounds. This trend is shown graphically in Fig. 3A and B, where the number of failed filters per compound among the full libraries and among the screening hits are displayed. For the confirmed hits the filtering results are biased by our cherry-picking procedure and the low structural diversity in case of the PCL compounds. However, especially in case of the confirmed hits of the MHC, the substantial number of failed filters per compound (2 ± 1, Tables 2 and 3) suggests that unspecific inhibitors are also present among the confirmed hits. Interestingly, a more than twofold increase in the failure rate of the Abbot ALARM
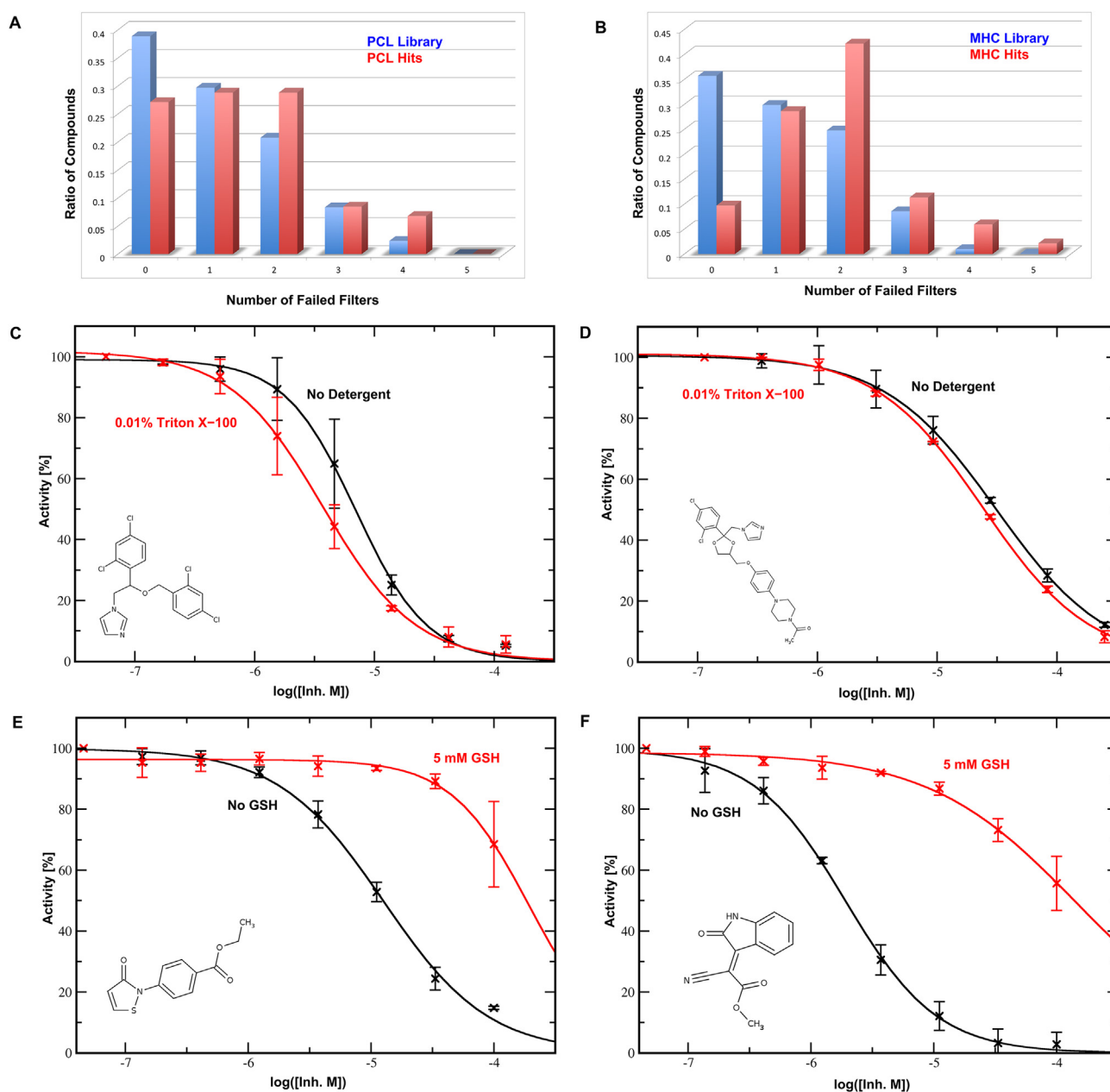
Fig. 3. Filtering results and dose—response curves of secondary enzymatic assays. Ratio of compounds that failed the indicated number of structural filters (0—5) (A) from the PCL library (blue) and its hits (red), and (B) from the MHC library (blue) and its hits (red). Enzymatic dose—response curves of (C) miconazole and (D) ketoconazole without (black) and with 0.01% Triton X-100 (red). Enzymatic dose—response curves of compounds (E) KM04550 and (F) S14435 without (black) and with (red) preincubation with 5 mM glutathione. (For interpretation of the references to color in this figure legend, the reader is referred to the web version of this article.)

filter is observed when passing from the full libraries (14% and 16%) to the screening hits (39% and 41%), suggesting that thiol reactivity plays a role in the detection of screening hits (Table 3).

The number of failed filters for each purchased screening hit is given in SI Tables S1 and S2.

2.5.2. Aggregators

Assay interference by aggregation has been extensively discussed in the literature over the last decade [28,38], but the detection of aggregation-prone compounds *in silico* remains challenging. Two algorithms developed in the Shoichet Laboratory [28,50] yield widely disparate results when filtering the MHC, the recursive partitioning filter [28] detecting 4825 compounds as possible aggregators, the similarity filter [50] detecting only 332 compounds, and the overlap between the two methods being only 117 compounds. However, experimentally the interference of aggregators can easily be minimized by the addition of small amounts of non-ionic detergent, which increases their IC_{50} values substantially [51,39]. Promiscuous aggregators often yield steep dose−response curves with large Hill slopes [38].

Counter-screening for aggregation-based inhibition was especially important for the imidazole antifungal agents, as three of them (miconazole, econazole, sulconazole) have been described as promiscuous aggregating inhibitors before, while another (keto-conazole) was not [28]. We therefore tested two of our antifungal agents, miconazole and ketoconazole, in the absence and in the presence of 0.01% Triton X-100 (Fig. 3C and D, Table 1). Interestingly, the dose−response curves of miconazole and ketoconazole display Hill slopes close to unity and do not shift to higher values in presence of detergent, as it would be expected for an aggregation-based inhibitor. We therefore propose that the imidazole antifungal agents act through a specific mechanism on IDO1.

We also tested most of the active compounds of the MHC for detergent-dependent inhibition (Table 2), including the three compounds (HTS01525, DP00477, NRB04258) that fail the stricter recursive partitioning filter for aggregators [28]. None of these compounds showed a significant increase of IC_{50} value characteristic for this type of promiscuous enzyme inhibition.

2.5.3. Chemically reactive compounds

Chemically reactive compounds may act on IDO1 activity not by specifically binding to its active site, but rather by reacting for example with the cofactors necessary for enzyme activation or with nucleophilic amino acid side chains. It has been shown, e.g., that the selenazal drug ebselen inhibits IDO1 by covalently modifying multiple cysteine residues [49].

The Lilly Medchem Rules [34] filter out 72% of the screening hits of the MHC, a 1.8-fold enrichment with respect to the ratio of failed compounds in the full library (Table 3). An even higher enrichment among the screening hits is observed for a number of specific exclusion rules, such as *quinone_para* (25.5-fold enrichment), *acyl_aromatic_nn* (7.9-fold), *hydrazone* (4.9-fold), *sulfonly_michael* (3.1-fold), *enamine* (2.9-fold), and *vinyl_cyano_2* (2.3-fold), all detecting potentially reactive compounds [34].

In order to experimentally test the prediction that some of the confirmed MHC hits could react with nucleophilic protein side chains, we carried out a secondary enzymatic assay, pre-incubating the compounds with high concentrations of glutathione (GSH) before adding IDO1 to the reaction mixture. Besides being a strong nucleophile, GSH is also a reducing agent. However, as the incubation medium already contained high concentrations of ascorbate, its reducing properties should have a minor influence on the enzymatic reaction. Indeed, the addition of GSH neither altered IDO1 activity, nor had it any effect on the measured IC_{50} value of the chemically inert compound 4-phenyl-imidazole (PIM). However, as

it is shown in Fig. 3E and F, preincubation with GSH strongly shifted the IC_{50} values of two electrophilic compounds, KM04550 and S14435, to higher concentrations. These results suggest that these compounds inhibit IDO1 through covalent modification of nucleophilic amino acid side chains. A similar trend was seen for compounds NRB00511, DP00477, and KM04416, which all failed at least the Lilly Medchem Rules or the Abbot ALARM thiol reactivity filter.

2.5.4. Redox-cycling compounds and para-quinones

Repetitively coupled reduction and oxidation reactions involving oxygen and reactive oxygen species are called "redox cycling". Redox-cycling compounds have been described as problematic compounds for HTS because of their appearance as false positives in many screens [29,36,37]. Since we observed numerous known redox-cycling compounds among our hits, we tried to determine if they inhibit IDO1 by entering into the active site and oxidizing active ferrous heme into inactive ferric heme (specific inhibition), or if they inhibit IDO1 by redox-cycling with the reducing cofactors in solution (ascorbate, methylene blue) to inactivate IDO1 (unspecific inhibition) [37]. This is an important question, not only for the interpretation of our HTS results, but also in view of the large number of published IDO1 inhibitors which contain a quinone or a quinone-like function [40,49,52−63]. The matter is complicated by the fact that quinones are not only redox-cycling compounds [64], but some are also chemically reactive towards nucleophilic amino acid side chains [32,65].

In the present HTS, 2 of the 7 *para*-quinones present in the PCL and 10 of the 29 *para*-quinones present in the MHC were classified as hits with the very high average score of 0.9 (SI Table S3). Structurally these compounds can be divided into benzoquinones (9 compounds, 2 hits), naphthoquinones (9 compounds, 7 hits), anthraquinones (15 compounds, 1 hit), and other quinones (3 compounds, 2 hits). In spite of the large structural diversity of the 12 active *para*-quinones, exemplified by their molecular weight (168−380 g/mol), number of rotatable dihedrals (0−12), number of hydrogen bond acceptors (2−6), and clogP (−2.1−3.6), their HTS scores only span the narrow range from 0.83 to 1.07 with two exceptions (0.62 and 0.60). This flat structure−activity relationship is indicative of an unspecific inhibition mechanism.

To address the question if there exists a correlation between redox potentials and HTS score, we calculated the redox potentials of all screening compounds by a semi-empirical quantum-chemical approximation. Additionally, the redox potentials of the 29 *para*-quinones present in the MHC were calculated by higher level density functional theory calculations (see SI for details). Indeed, the calculations showed that on average the screening hits are more prone to redox cycling than the inactive compounds, but the differences are statistically not significant (Fig. S1A). For the *para*-quinones, we did not find a correlation between their oxidation potential and the HTS score (Fig. S1B). A similar absence of correlation between calculated oxidation potentials and redox-cycling activity has recently been found in a screening specifically designed to detect redox-cycling compounds [64]. These findings suggest that the chemical reactivity of quinones [32,65] must also be taken into account. In fact, the 29 *para*-quinones on average failed 4.3 out of the five structural filters we applied (Table S3). It seems common medicinal chemistry knowledge that quinones do not present valid lead-like properties.

2.6. Lead optimization of the imidazole antifungal agents

The high and uniform activity of the imidazole antifungal agents in the enzymatic assay (Table 1) is remarkable, especially when confronted with the complete inactivity of the structurally very similar class of 1,2,4-triazole antifungal drugs (anastrozole,

Table 4
Derivatives of the imidazole antifungal scaffold. The modified part according to the IDO1-binding analysis, the respective substitutions, and the enzymatic IC_{50} values are indicated. NI: no inhibition.
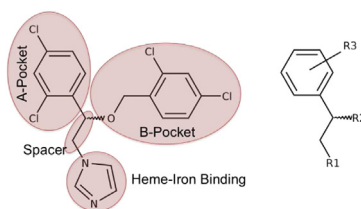
Comp.	Modification	R1	R2	R3	Enz. IC_{50} [µM]
2	A	Compound = (structure)			NI
4a	B	Imidazol-1-yl	H	2,4-di-Cl	820
4b	A + B	Imidazol-1-yl	H	–	NI
6a	B	Imidazol-1-yl	OCH_3	2,4-di-Cl	140
6b	B	Imidazol-1-yl	OCH_2-3-pyridyl	2,4-di-Cl	84
7	B	Imidazol-1-yl	=O	2,4-di-Cl	NI
10a	B	Imidazol-1-yl	OH	2,4-di-Cl	130
10b	A + B	Imidazol-1-yl	OH	–	NI
10c	A + B	Imidazol-1-yl	OH	2-Cl	200
10d	A + B	Imidazol-1-yl	OH	3,4-di-Cl	830
10e	A + B	Imidazol-1-yl	OH	3-Cl	NI
10f	A + B	Imidazol-1-yl	OH	4-Cl	NI
10g	A + B	Imidazol-1-yl	OH	2,6-di-Cl	NI
10h	A + B	Imidazol-1-yl	OH	2-OH	NI
10i	Heme	1,2,4-Triazol-1-yl	OH	2,4-di-Cl	NI
13	Heme	1,2,3-Triazol-4-yl	OH	2,4-di-Cl	NI
4c	Spacer + B	Compound = (structure)			310
15	Spacer + B	Compound = (structure)			NI
16	Spacer + A + B	Compound = (structure)			NI
17	Spacer + A + B	Compound = (structure)			NI

fluconazole, itraconazole, letrozole, terconazole, voriconazole) also present among the screening compounds. This striking difference between the imidazole and the 1,2,4-triazole heterocycle is reminiscent of the discrimination of IDO1 between the regioisomers 4-phenyl-1,2,3-triazole (enzymatic $IC_{50} = 83$ µM) and 3-phenyl-1,2,4-triazole (no inhibition) [41]. Together with the known binding mode of imidazole antifungal drugs to the iron of heme proteins via their unsubstituted imidazole nitrogen, resolved in many X-ray structures [46], this finding suggests that also in IDO1 the imidazole ring binds directly to the heme iron. As we described above, testing of representative members of the imidazole antifungal agents for aggregation-based inhibition returned negative results, suggesting that they inhibit IDO1 through a specific mechanism. Although the cellular IC_{50} values of the antifungal agents could not be determined due to their high toxicity in the MTS/PMS cell viability assay, we selected this scaffold for optimization, expecting that the cytotoxicity issue may be resolved based on the low number of structural alerts (Table 1). Imidazoles substituted on the carbon

atom in position four have been described previously as IDO1 inhibitors [66–68]. Recently, also 4,5-disubstituted imidazoles active on IDO1 have been discovered [69]. Here, we explore for the first time the structure–activity relationship of 1-substituted imidazoles.

2.6.1. In silico studies

To date only two X-ray structures of IDO1 have been published, one with cyanide and the other with the inhibitor 4-phenyl-imidazole (PIM) bound to the heme iron [70]. The latter has successfully been used by ourselves [40,41] and by others [66,71,72] for the structure-based design of new IDO1 inhibitors. In order to guide lead optimization, we attempted to dock the imidazole antifungal agents into the IDO1 active site. However, since PIM is much smaller, there is not enough space in the corresponding X-ray structure to fit the larger antifungal agents.

We therefore modeled the induced fit resulting from imidazole antifungal agent binding by carrying out molecular dynamics (MD)

simulations of fully solvated IDO1 with miconazole bound in a putative binding mode, and slowly removing all restraints such as to obtain an intrinsically stable complex. The initial binding mode of miconazole was chosen similar to the binding modes of imidazole antifungal agents in CYP proteins, with the free imidazole nitrogen bound to the heme iron, one of its chlorinated phenyl rings extending into the hydrophobic and buried A pocket, and the other into the B pocket at the entrance of the active site.
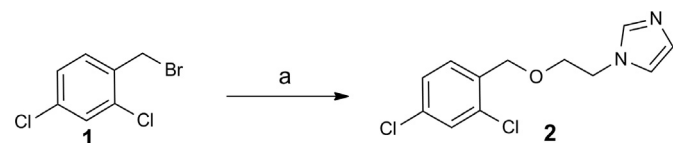
In order to accommodate miconazole, IDO1 undergoes slight structural rearrangements which increase the size of pocket A, but the overall backbone displacements remain small (RMSD = 0.95 ± 0.09 Å for the residues within 5 Å of the ligand). Miconazole rearranges undergoing several dihedral transitions to accommodate one phenyl ring deeper in pocket A and the other one deeper in pocket B. In this conformation it remains stable without constraints for several tens of nanoseconds (Fig. 2B).

Using the central structure of the stable conformation of miconazole from the MD simulations for docking with EADock-DSS [73], a consistent binding mode for all antifungal agents was found, with the imidazole bound to the heme iron, the phenyl ring deeply buried inside the A pocket, and the second aromatic or conjugated moiety located in the B pocket (Fig. 2B–I). Miconazole, as many other imidazole antifungal agents, possesses a chiral center. However, both enantiomers can bind to the IDO1 active site in a very similar manner (Fig. 2B, C).
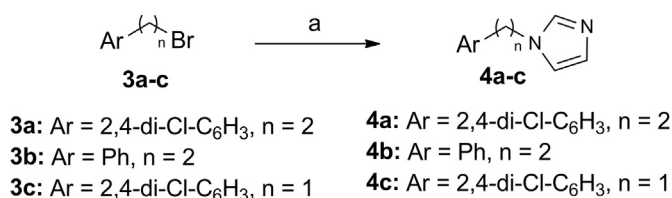
Based on the docked structures of the antifungal agents, we divided the representative structure of miconazole (IC$_{50}$ = 7.6 μM) into four structural entities: a heme binding motif (imidazole), a spacer, an aromatic moiety occupying the A pocket, and an aromatic moiety occupying the B pocket (Table 4). All active antifungal agents share the same heme binding motif, and, except for bifonazole, all share the same spacer and A-pocket moiety. The greatest structural variety is seen in the B pocket moiety.

2.6.2. Synthesis

The derivatives of the imidazole antifungal agents were synthesized using previously published protocols or procedures adapted from the literature [(2, 6a–6b) [74], (4a–4c) [75], (10a–10i) [74,76], (13) [77,78] (15) [79]]. Compound 2 was obtained by treatment of 2,4-dichlorobenzyl bromide with 2-(1H-imidazol-1-yl)ethanol and sodium hydride in THF (Scheme 1). Compounds 4a–4c were obtained by treatment of an aryl bromide with imidazole and potassium carbonate in THF (Scheme 2). Compounds 6a–6b were prepared by reaction of the 1-(2,4-dichlorophenyl)-2-(1H-imidazol-1-yl)ethanol with alkyl and aryl halides (Scheme 3). A series of target compounds, namely the 1-aryl-2-(1H-imidazol-1-yl)ethanols (10a–10h) and 1-(2,4-dichlorophenyl)-2-(1H-1,2,4-triazol-1-yl)ethanol (10i) were prepared by reaction of the respective 1-aryl-2-bromoethanones with imidazole/1H-1,2,4-triazole (Schemes 4 and 5). Most of the required 1-aryl-2-bromoethanones were commercially available. Compound 13 was obtained by allylation of 2,4-dichlorobenzaldehyde with propargylbromide mediated by zinc powder. The resulting ethynyl derivative was reacted with TMSN$_3$ (Scheme 6). Compound 15 was obtained by treatment of 2,4-dichloro-1-fluorobenzene with 1-

3a: Ar = 2,4-di-Cl-C$_6$H$_3$, n = 2　　4a: Ar = 2,4-di-Cl-C$_6$H$_3$, n = 2
3b: Ar = Ph, n = 2　　　　　　　　　4b: Ar = Ph, n = 2
3c: Ar = 2,4-di-Cl-C$_6$H$_3$, n = 1　　4c: Ar = 2,4-di-Cl-C$_6$H$_3$, n = 1

Scheme 2. Reagents & conditions: (a) Imidazole, K$_2$CO$_3$, THF, reflux, 14 h.

(trimethylsilyl)-1H-imidazole and CsF in DMF (Scheme 7). All other compounds (7, 16, 17) were bought from Sigma–Aldrich.
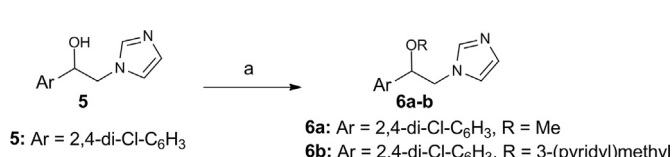
2.6.3. Structure–activity relationship

In order to establish a structure–activity relationship and to increase the solubility of the imidazole antifungal family, we chemically modified all four elements of the scaffold separately and in combination (Table 4). All IC$_{50}$ determinations were carried out in the presence of 0.01% of Triton X-100 to minimize aggregation-based inhibition.

Complete removal of the A-pocket group resulted in an inactive compound (2), while complete removal of the B-pocket group resulted in a compound with weak but detectable activity (4a, IC$_{50}$ = 820 μM). Replacement of the aromatic B-pocket moiety by a 3-pyridyl group (6b) yielded a compound with an IC$_{50}$ value of 84 μM. Limitation of the B-pocket group to the methoxy (6a, IC$_{50}$ = 140 μM) or to the hydroxyl function (10a, IC$_{50}$ = 130 μM) both yielded active compounds, while the corresponding keto compound (7) was inactive. All these derivatives showed the advantage of substantially enhanced solubility (>1 mM) with respect to miconazole (≈10 μM). While improving solubility, modifications of the B-pocket group lowered the activity ten to twenty-fold. However, this region seems to be amenable to optimizations and can be explored further.
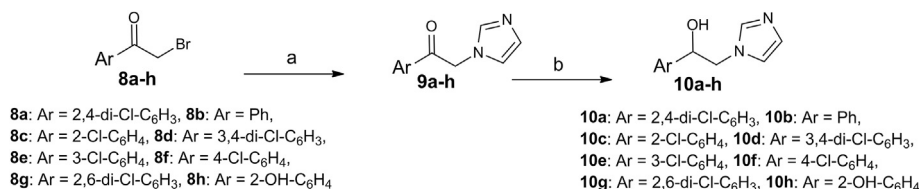
Other modifications of the A-pocket group were tested on compounds also lacking the aromatic B-pocket group in order to profit from improved solubility. Removal of both chloride substituents from the A-pocket phenyl ring lead to an inactive compound (10b) while removal of the 4-Cl substituent alone (10c) yielded an active compound with an IC$_{50}$ value of 200 μM. Other substitutions on the phenyl ring in pocket A yielded less active (10d, IC$_{50}$ = 830 μM) or inactive compounds (10e, 10f, 10g, 10h).

Modification of the heme-binding moiety from imidazole to either 1,2,4-triazole (10i) or 1,2,3-triazole (13) completely abolished activity, suggesting that the 1,2,4-triazole antifungal drugs present in the PCL are indeed inactive because of their heme-binding moiety. Removal of the B-pocket group and simultaneous shortening of the spacer from two carbon atoms to one carbon atom (4c) yielded a compound which was about 2.5 fold more active than the corresponding compound with the original spacer (4a). However, complete elimination of the spacer (15) yielded an inactive compound. Elimination of the di-chloride substitution in pocket A of the shortened compounds yielded inactive compounds (16 and 17), in agreement with the inactivity of compound 4b.

In summary, our studies demonstrate that (i) the heme-binding moiety is essential for activity, (ii) the spacer may be shortened from two to one carbon atom, (iii) the A-pocket is sensitive to the di-

**Scheme 1.** Reagents & conditions: (a) 2-(1H-imidazol-1-yl)ethanol, NaH, THF, reflux, 3 h.

5: Ar = 2,4-di-Cl-C$_6$H$_3$

6a: Ar = 2,4-di-Cl-C$_6$H$_3$, R = Me
6b: Ar = 2,4-di-Cl-C$_6$H$_3$, R = 3-(pyridyl)methyl

Scheme 3. (a) NaH, RX, DMF, 0 °C-rt, 1.5 h.

8a: Ar = 2,4-di-Cl-C$_6$H$_3$, **8b**: Ar = Ph,
8c: Ar = 2-Cl-C$_6$H$_4$, **8d**: Ar = 3,4-di-Cl-C$_6$H$_3$,
8e: Ar = 3-Cl-C$_6$H$_4$, **8f**: Ar = 4-Cl-C$_6$H$_4$,
8g: Ar = 2,6-di-Cl-C$_6$H$_3$, **8h**: Ar = 2-OH-C$_6$H$_4$

10a: Ar = 2,4-di-Cl-C$_6$H$_3$, **10b**: Ar = Ph,
10c: Ar = 2-Cl-C$_6$H$_4$, **10d**: Ar = 3,4-di-Cl-C$_6$H$_3$,
10e: Ar = 3-Cl-C$_6$H$_4$, **10f**: Ar = 4-Cl-C$_6$H$_4$,
10g: Ar = 2,6-di-Cl-C$_6$H$_3$, **10h**: Ar = 2-OH-C$_6$H$_4$

Scheme 4. Reagents & conditions: (a) Imidazole, K$_2$CO$_3$, DMF, rt, 2–3 h (b) NaBH$_4$, MeOH, 0 °C-rt-50 °C 2 h.
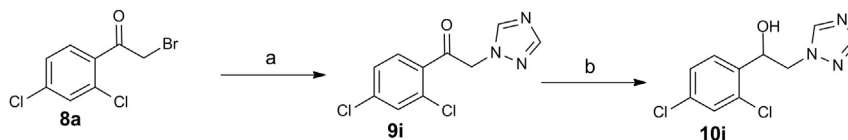
Scheme 5. Reagents & conditions: (a) 1H-1,2,4-triazole, K$_2$CO$_3$, DMF, rt, 2–3 h (b) NaBH$_4$, MeOH, 0 °C-rt-50 °C 2 h.
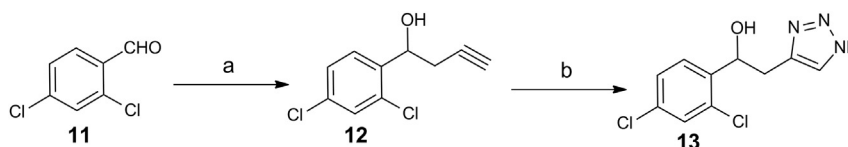
Scheme 6. Reagents & conditions: (a) propargylbromide, Zn powder, 1 h (b) TMSN$_3$, CuI, DMF/MeOH (9:1), 100 °C, 10–12 h.

chloride substitutions in the right place, (iv) the B-pocket group is most amenable to optimization, and (v) removal of one of the aromatic moieties from the A pocket or the B pocket greatly enhances solubility. The fact that we obtained a structure–activity relationship covering an activity range of more than three orders of magnitude suggests that the imidazole antifungal scaffold is amenable to optimization and inhibiting IDO1 through a specific mechanism.

3. Conclusions

We have screened a library of FDA-approved compounds and a library of drug-like compounds for IDO1 inhibition. The screening assay was based on a commonly used enzymatic assay protocol and displayed a good sensitivity and robustness, expressed in a cumulative interplate Z' of 0.8. However, of the 60 hit compounds selected for follow-up studies, an enzymatic IC$_{50}$ value could be determined only for 21 of them, and only four were active in cellular assays. Through experimental and computational studies we could show that most of the screening hits inhibit IDO1 through unspecific inhibition mechanisms such as covalent reactivity or redox cycling.

The only compound inhibiting mIDO1 but not mTDO in a cellular context was the MHC compound CD02761 (Table 2). However, this compound was flagged as problematic by 3 out of 5 structural filters because of its isothiourea functionality. S-substituted isothioureas have been described before as IDO1 inhibitors in enzymatic and cellular assays [80], but their activities might be influenced by hydrolysis to the corresponding reactive thiols, which were also shown to be active [80].

Some FDA-approved compounds from the PCL showed confirmed IDO1 inhibitory activity, for example phenelzine, a non-selective and irreversible monoamine oxidase inhibitor which is used as an antidepressant and anxiolytic. Recently, similar hydrazines have been described as IDO inhibitors [25]. However, phenelzine has been suggested to covalently bind to the porphyrin of the heme prosthetic group of CYP, thereby destroying it [47]. Moreover, the maximal daily dose of phenelzine (75–90 mg) might not be enough for significant IDO1 inhibition in vivo.

The imidazole antifungal agents described here provide a specific IDO1 inhibiting scaffold. Most of these compounds are only approved

for topical application, but they might still be interesting in the local treatment of certain cancer types, such as melanoma for instance. The reported therapeutic concentrations for example for miconazole (40 μM) and econazole (26 μM) [28] are larger than their determined IC$_{50}$ values on IDO1 and could therefore induce significant IDO1 inhibition in vivo. Here, the imidazole antifungal scaffold was chosen for rational structure-based lead optimization, which led to more soluble and smaller compounds with micromolar activity.

In summary, despite the robust screening results based on the well-established enzymatic assay protocol for IDO1, most screening hits turned out to be false positives or unspecific inhibitors, establishing IDO1 as a difficult screening target. We hope that the present work will be useful for other researchers in the field to critically assess the specificity of novel IDO1 inhibitors.

4. Methods

4.1. HTS assay

The HTS was carried out on Corning UV-transparent flat-bottom 384-well plates. The reaction mixture (80 μl) contained potassium phosphate buffer at pH 6.5 (50 mM), ascorbic acid as reductant (10 mM), methylene blue as electron-carrier (5 μM), the substrate L-Trp (100 μM), the tested compound (10 μM), DMSO (1%), and IDO1 (4 μg/mL). Before starting the incubation by addition of IDO1, the absorbance of each reaction well was recorded at a wavelength of 320 nm. After incubation at room temperature for 60 min, the reaction was stopped by addition of hydrogen peroxide solution (8 μl, 1 M), and absorbance at 320 nm was remeasured. The
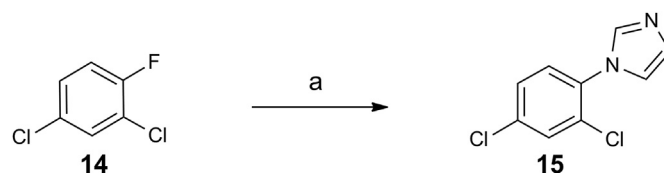
Scheme 7. Reagents & conditions: (a) 1-(trimethylsilyl)-1H-imidazole, CsF, DMF, 60 °C, 20 h.

screening was carried out in duplicates. On each plate, 64 wells were reserved for control samples.

The change in absorbance at 320 nm before and after incubation with IDO1 is expected to be proportional to the quantity of NFK formed by the enzymatic oxidation of L-Trp by IDO1 and thus yields a measure of IDO1 activity in presence of the tested compound.

4.2. In vitro assay

The enzymatic assay was carried out on 96-well plates. The reaction mixture (100 μl) contained potassium phosphate buffer at pH 6.5 (100 mM), ascorbic acid as reductant (20 mM), methylene blue as electron carrier (10 μM), bovine catalase to remove hydrogen peroxide (400 units/mL), the substrate L-Trp (100 μM), the screening compound at varying concentrations, DMSO (5%), and IDO1 (2.5 μg/mL). After incubation at room temperature for 60 min, the reaction was stopped by addition of trichloroacetic acid solution (40 μl, 30% w/v), and the samples were incubated at 50 °C for 30 min to allow hydrolysis of the enzymatic reaction product, NFK, to kynurenine. After centrifugation, 80 μl of supernatant from each well were used for HPLC analysis.

The mobile phase for HPLC analysis was composed of 50% (v/v) of methanol and 50% of sodium citrate buffer (40 mM, pH 2.35) containing 400 μM sodium dodecyl sulfate. An Agilent Zorbax Eclipse XDB C18 column (150 × 4.6 mm) was used at 23 °C with a flow rate of 1 mL/min and an injection volume of 20 μl. For detection of kynurenine, absorption at 365 nm was measured, while remaining L-Trp was detected at a wavelength of 280 nm. All assays were carried out in duplicates.

4.3. Cellular assays

For evaluating inhibition of murine IDO1 and murine TDO in a cellular context, we used cell lines P815-mIDO1 clone 6 and P815-mTDO clone 12, respectively, as described in Ref. [40]. The inhibition assays were performed in 96-well flat bottom plates seeded with 2×10^5 cells in a final volume of 200 μl of IMDM (Iscove's Modified Dulbecco's Medium, Invitrogen) (80 μM L-tryptophan) supplemented with 2% FCS and a titration of the compound ranging from 0.024 to 25 μM. The cells were incubated at 37 °C for 18 h (mIDO1) or for 24 h (mTDO). The reaction was stopped before 50% of the initial amount of tryptophan was converted into kynurenine to assure linearity of the reaction. The plates were then centrifuged for 10 min at 300 g, and 150 μl of the supernatant were collected for HPLC analysis of tryptophan and kynurenine concentrations. Proteins were precipitated by mixing 50 μl of supernatant with an equal volume of TCA 6%. After centrifugation, 70 μl of supernatant were collected, diluted in an equal volume of water and injected into the HPLC system (C18 column). Tryptophan was detected at an absorption wavelength of 280 nm, and kynurenine at 360 nm.

To estimate cytotoxicity (LD_{50}), 2×10^5 P815 cells were plated in 96-well flat bottom plates in a final volume of 200 μl of IMDM (Invitrogen) supplemented with 2% FCS and a titration of the compound ranging from 0.024 to 25 μM. After 24 h of incubation at 37 °C, the number of living cells was evaluated with a MTS/PMS assay (Promega) as described by the manufacturer.

4.4. Structural filtering of screening compounds

We used the implementation of the Lilly Medchem Rules [34] provided by one of the original authors which is available free of charge at http://github.com/IanAWatson/Lilly-Medchem-Rules. The PAINS filter (Tables S6–S8 from the original reference [33]) was applied within the Filter-it software from Silicos-it (http://silicos-it.com/), using the SMARTS list from Chris Swain (http://www.

macinchem.org/reviews/pains/painsFilter.php). The Pfizer LINT [31], Abbot ALARM [32], and Glaxo [30] filter calculations were performed through the SmartsFilter web application, kindly provided by the Division of Biocomputing, Dept. of Biochemistry & Molecular Biology, University of New Mexico, Albuquerque, NM, (http://pasilla.health.unm.edu/tomcat/biocomp/smartsfilter). For the Abbot ALARM filter, we used a lower cutoff of 0.3 for the thiol reactivity index [32]. For the Glaxo filter, the three subfilters for reactive functional groups, unsuitable leads, and unsuitable natural products [30] were considered as a single filter. The detection of aggregators based on the recursive partitioning filter [28] was used as implemented in FILTER version 2.0.2. from OpenEye Scientific Software, Santa Fe, NM. The detection of aggregators based on similarity to known aggregators [50] is available through the "Aggregator Advisor" web service (http://advisor.bkslab.org).

4.5. Modeling

We docked the hits of the two compound libraries *in silico* into the IDO1 active site as provided in the PIM-bound X-ray structure (PDB: 2D0T, chain A) [70].

A consensus docking procedure based on our in-house docking algorithms EADock [81–83], EADock DSS [73] and AttractingCavities [84] was used. All three algorithms rely on the physical scoring function of the CHARMM22 force field [85], while solvation effects are taken into account by the FACTS model [86], which has been shown to allow for accurate docking results [87]. Ligand force-field parameters were derived with the SwissParam tool [88]. A Morse-like metal binding potential (MMBP) was used to describe the interactions between the heme iron of IDO1 and ligand atoms that display a free electron pair for iron binding [89]. Two molecules of N-cyclohexyltaurine bound at the entrance of the binding site [70] were removed during setup, and the protein was kept fixed during docking. For more details see Ref. [41].

An induced-fit structure of miconazole bound to IDO1 was created by relaxing the protein structure around a putative binding mode of the antifungal agent, forcing one phenyl ring into pocket A, the other one into pocket B, and the imidazole binding to the heme iron. We carried out MD simulations of the IDO1/miconazole complex using the GROMACS code version 4.5.1 [90] in combination with the all-atom CHARMM27 force field [91,92] and the explicit TIP3P water model [93]. A neutral system at physiological ion concentration (≈ 150 mmol/L) was obtained by adding sodium and chloride ions. The box dimension of $(100 \text{ Å})^3$ was chosen so that the initial minimum gap between periodic images of the protein was 30 Å. Electrostatic interactions were calculated with the particle mesh Ewald method [94]. Bonds involving hydrogen atoms were constrained using the P-LINCS algorithm [95]. The time integration step was set to 2 fs. The system was kept at ambient temperature (300 K) through velocity rescaling with a relaxation time of 0.2 ps [96] and at ambient pressure (1 bar) by coupling to a Berendsen bath [97] with a relaxation time of 1 ps. A distance restraint between the heme iron and the available imidazole nitrogen of miconazole served to mimic a covalent bond.

The whole system was energy minimized, heated to 300 K over a period of 100 ps, and equilibrated for 900 ps at 300 K, restraining protein heavy atoms to their positions in the X-ray structure. For a further 10 ns, only the positions of the heme and the ligand heavy atoms were restrained to their initial positions, before removing all structural restraints and continuing the simulation for another 10 ns.

4.6. Calculation of redox potentials

For the two libraries of 15,200 compounds in total, we optimized the molecular geometries in gas phase with the semi-

empirical AM1 method [98] using the Gaussian09 code [99]. Their reduction and oxidation potentials were approximated by the resulting HOMO and LUMO energies, as described before [100]. We checked that the inclusion of implicit aqueous solvation with the conductor-like polarizable continuum model (CPCM) [101,102] did not change the results qualitatively.

For more detailed calculations on the 29 *para*-quinones of the MHC, we adapted a recently reported procedure [103]. Each compound was geometry optimized in the gas phase both in its oxidized and in its one-electron reduced state at the density functional theory level using the B3LYP hybrid functional [104,105] and the 6-31G(d) basis set in the Gaussian09 code [99]. Aqueous-phase molecular energies were calculated by using the conductor-like polarizable continuum model (CPCM) [101,102] with its default settings. It has been shown that the difference between the solution-phase molecular energies of the reduced and the oxidized species are highly correlated with experimentally measured reduction potentials [103]. As reported recently, the energy difference computed in this way is highly correlated with the LUMO energy of the oxidized compound [106] thus reducing the necessary calculations per compound from four to two.

4.7. Chemistry

4.7.1. General remarks

Materials and reagents were obtained from commercial suppliers and used without further purification. For extraction and chromatography, all solvents were distilled prior to use. Thin layer chromatography for reaction monitoring was performed on silica gel plates (Merck 60 F254) with detection by UV light (254 nm) and charring with KMnO$_4$ or Pancaldi reagent. Flash chromatography was conducted using silica gel 60 Å, 230–400 mesh (Merck 9385). Melting points were measured with a Mettler FP52 apparatus and are uncorrected. IR spectra were recorded on a Perkin–Elmer Paragon 1000 FT-IR spectrometer. Mass spectra were recorded on a Nermag R 10-10C instrument in chemical ionization mode. Electrospray mass analyses were recorded on a Finnigan MAT SSQ 710C spectrometer in positive ionization mode. ^{1}H and ^{13}C NMR spectra were recorded Bruker-DPX-400 or Bruker-ARX-400 spectrometer at 400 MHz and 100.6 MHz, respectively. Data for ^{1}H NMR spectra are reported as follows: chemical shift, multiplicity, coupling constant, and integration. Data for ^{13}C NMR spectra are reported in terms of chemical shifts. Chemical shifts are given in parts per million, relative to an internal standard such as residual solvent signals. Coupling constants are given in Hertz. High-resolution mass spectra were recorded via ESI-TOF-HRMS. The purity of all novel compounds was confirmed to exceed 95% by NMR and high-resolution mass spectra.

4.7.2. Procedures
4.7.2.1. 1-(2-((2,4-Dichlorobenzyl)oxy)ethyl)-1H-imidazole (2).
A suspension of sodium hydride (2 mmol, 2 eq) in THF (5 mL) was treated with a solution of 2-(1H-imidazol-1-yl)ethanol (1 mmol, 1 eq) in THF (3 mL) at 0 °C. The resulting mixture was stirred under a nitrogen atmosphere at room temperature for 1 h. The mixture was cooled to 0 °C before addition of 2,4-dichlorobenzyl bromide (1, 1.5 mmol, 1.5 eq). The resulting mixture was stirred under reflux for 3 h. The reaction was quenched by addition of a saturated aqueous solution of NH$_4$Cl (5 mL). The aqueous phase was extracted with ethyl acetate (15 mL, three times), the organic phase was washed with water (10 mL), dried over Na$_2$SO$_4$ and the solvent was removed in vacuo. Purification by column chromatography (SiO$_2$, MeOH/ethyl acetate) afforded **2** as an oil in 65% yield. IR (film): ν_{max}: 3109, 2868, 1898, 1589, 1505, 1469, 1075, 813, 737 cm^{-1}. ^{1}H NMR (400 MHz, CDCl$_3$): δ 7.55 (bs, 1H), 7.37 (s, 1H), 7.24–7.23 (m, 2H),

7.07 (bs, 1H), 6.98 (s, 1H), 4.56 (s, 2H), 4.17 (t, 2H, *J* = 5.1 Hz), 3.79 (t, 2H, *J* = 5.1 Hz) ppm. ^{13}C NMR (100 MHz, CDCl$_3$): δ 137.5, 133.9, 133.88, 133.3, 129.6, 129.4, 129.1, 127.0, 119.4, 70.0, 69.6, 47.0 ppm. ESI-TOF-HRMS: *m/z* calcd for (M + H) C$_{12}$H$_{12}$N$_2$Cl$_2$O 271.0405 found 271.0416.

4.7.2.2. 1-(2,4-Dichlorophenethyl)-1H-imidazole (*4a*) [107].
Under a nitrogen atmosphere, a mixture of imidazole (2.1 mmol, 2.1 eq) and K$_2$CO$_3$ (1 mmol, 1 eq) in dry THF (6 mL) was stirred at room temperature for 10 min. A solution of 1-(2-bromoethyl)-2,4-dichlorobenzene (**3a**, 1 mmol, 1 eq) in THF (1 mL) was added, and the mixture was heated under reflux for 14 h. The solution was filtered and the filtrate was concentrated in vacuo. The residue was dissolved in CH$_2$Cl$_2$, and the solution was washed with water (5 mL, twice). The CH$_2$Cl$_2$ layer was extracted with dilute aqueous HCl (5 mL, three times). The aqueous extract was neutralized with solid NaHCO$_3$, and the free base was extracted using CH$_2$Cl$_2$ (10 mL, three times). The combined organic extracts were dried (Na$_2$SO$_4$) and concentrated. High-vacuum drying gave **4a** as an oil in 45% yield. ^{1}H NMR (400 MHz, CDCl$_3$): δ 7.44–7.42 (m, 1H), 7.33 (s, 1H), 7.14 (dd, 1H, *J* = 8.2, *J* = 2.2 Hz), 7.05 (bs, 1H), 6.88 (d, 1H, *J* = 8.0 Hz), 6.85 (s, 1H), 4.20 (t, 2H, *J* = 7.0 Hz), 3.16 (t, 2H, *J* = 7.0 Hz) ppm.

4.7.2.3. 1-Phenylethyl-1H-imidazole (*4b*) [75].
Same procedure as for the preparation of **4a**, using imidazole and (2-bromoethyl) benzene (**3b**) affords **4b** as an oil in 42% yield. ^{1}H NMR (400 MHz, CDCl$_3$): δ 7.33–7.22 (m, 4H), 7.09–7.02 (m, 3H), 6.83 (s, 1H), 4.17 (t, 2H, *J* = 7.0 Hz), 3.05 (t, 2H, *J* = 7.0 Hz) ppm.

4.7.2.4. 1-(2,4-Dichlorobenzyl)-1H-imidazole (*4c*) [108].
Same procedure as for the preparation of **4a**, using imidazole and 1-(bromomethyl)-2,4-dichlorobenzene (**3c**) affords **4c** as a white solid in 60% yield. ^{1}H NMR (400 MHz, CDCl$_3$): δ 7.59 (s, 1H), 7.47 (d, 1H, *J* = 2.2 Hz), 7.25 (dd, 1H, *J* = 8.2, *J* = 2.6 Hz), 7.15 (bs, 1H), 6.96 (bs, 1H), 6.88 (d, 1H, *J* = 8.0 Hz), 5.22 (s, 2H) ppm.

4.7.2.5. 1-(2-(2,4-Dichlorophenyl)-2-methoxyethyl)-1H-imidazole (*6a*) [109].
A suspension of sodium hydride (1.5 mmol, 1.5 eq) in DMF (5 mL) was treated with a solution of 1-(2,4-dichlorophenyl)-2-(1H-imidazol-1-yl)ethanol (**5**, 1 mmol, 1 eq) in DMF (5 mL) at 0 °C. The resulting mixture was stirred under a nitrogen atmosphere at room temperature for 1.5 h. The mixture was cooled to 0 °C and methyliodide (1 mmol, 1 eq) was added. The resulting mixture was stirred for 1 h at room temperature. The reaction was quenched by addition of water (15 mL). The aqueous phase was extracted with ethyl acetate (15 mL, three times), the organic was washed with water (15 mL), dried over Na$_2$SO$_4$ and the solvent was removed in vacuo. Purification by column chromatography (SiO$_2$, MeOH/ethyl acetate) afforded **6a** as an oil in 60% yield. ^{1}H NMR (400 MHz, CDCl$_3$): δ 7.48–7.42 (m, 2H), 7.30–7.21 (m, 2H), 7.03 (bs, 1H), 6.92 (s, 1H), 4.78 (dd, 1H, *J* = 7.0, *J* = 2.6 Hz), 4.21–4.16 (m, 1H), 4.04–3.97 (m, 1H), 3.25 (s, 3H) ppm.

4.7.2.6. 3-((1-(2,4-Dichlorophenyl)-2-(1H-imidazol-1-yl)ethoxy) methyl)pyridine (*6b*).
Synthesized from **5** and 3-(bromomethyl) pyridine using the same procedure as for **6a** to afford **6b** as an oil in 62% yield. IR (film): ν_{max}: 3366, 2923, 2868, 1918, 1717, 1588, 1504, 1468, 1229, 1090, 786 cm^{-1}. ^{1}H NMR (400 MHz, CDCl$_3$): δ 8.56 (dd, 1H, *J* = 5.0, *J* = 1.5 Hz), 8.45 (s, 1H), 7.49–7.44 (m, 3H), 7.35–7.24 (m, 3H), 7.04 (bs, 1H), 6.90 (s, 1H), 4.99 (dd, 1H, *J* = 7.6, *J* = 2.6 Hz), 4.50–4.45 (m, 1H), 4.30–4.18 (m, 2H), 4.09–4.01 (m,1H) ppm. ^{13}C NMR (100 MHz, CDCl$_3$): δ 149.3, 148.8, 137.7, 135.5, 135.1, 133.6, 133.3, 132.4, 129.7, 129.0, 128.4, 128.0, 123.7, 119.8, 69.1, 51.3 ppm. ESI-TOF-HRMS: *m/z* calcd for (M + H) C$_{17}$H$_{15}$N$_3$OCl$_2$ 348.0670 found 348.0684.

4.7.2.7. General procedure for the synthesis of imidazole alcohols (10a–10h). A mixture of the α-bromoketone (**8a–h**, 1 mmol, 1 eq), imidazole (3 mmol, 3 eq), and anhydrous K_2CO_3 (3 mmol, 3 eq) in DMF (3 mL) was stirred at room temperature for 2–3 h. The reaction mixture was diluted with H_2O (10 mL) and extracted with EtOAc (15 mL, twice). The combined organic phase was washed sequentially with H_2O (10 mL) and brine (10 mL). The combined organic extracts were dried over Na_2SO_4, and evaporated. High-vacuum drying gave crude **9a–h**. A solution of crude **9a–h** (1 mmol, 1 eq) in methanol (4 mL) was added to a suspension of sodium borohydride (1 mmol, 1 eq) in anhydrous methanol (20 mL) maintaining the temperature below 5 °C under atmospheric pressure. The resulting mixture was stirred at room temperature for 1 h and then heated to 50 °C for 1 h. After cooling to room temperature the reaction mixture was concentrated and water (8 mL) was added. The product was extracted with ethyl acetate (10 mL, twice). The organic phase was dried over Na_2SO_4 and purified by flash chromatography on silica gel using MeOH–EtOAc (6:94) as the eluent to afford the imidazole alcohol (**10a–10h**); overall yields up to 77%.

4.7.2.8. 1-(2,4-Dichlorophenyl)-2-(1H-imidazol-1-yl)ethanol (10a) [110]. Synthesized from 2-bromo-1-(2,4-dichlorophenyl)ethanone (**8a**) according to the general procedure to afford **10a** as a white solid in 75% yield, ^{1}H NMR (400 MHz, CDCl₃): δ 7.61–7.57 (m, 1H), 7.44–7.39 (m, 2H), 7.34–7.30 (m, 1H), 6.93 (s, 1H), 6.92–6.87 (m, 1H), 5.30–5.25 (m, 1H), 4.28–4.20 (m, 1H), 3.94–3.85 (m, 1H) ppm.

4.7.2.9. 2-(1H-imidazol-1-yl)-1-phenylethanol (10b) [111]. Synthesized from 2/bromo/1/phenylethanone (**8b**) according to the general procedure to afford **10b** as a white solid in 70% yield, ^{1}H NMR (400 MHz, CDCl₃): δ 7.43–7.29 (m, 6H), 7.02 (bs, 1H), 6.92 (s, 1H), 4.98–4.93 (m, 1H), 4.20–4.08 (m, 2H) ppm.

4.7.2.10. 1-(2-Chlorophenyl)-2-(1H-imidazol-1-yl)ethanol (10c) [112]. Synthesized from 2-bromo-1-(2-chlorophenyl)ethanone (**8c**) according to the general procedure to afford **10c** as a white solid in 72% yield, ^{1}H NMR (400 MHz, CDCl₃): δ 7.60–7.54 (m, 2H), 7.40–7.37 (m, 1H), 7.35–7.27 (m, 2H), 7.02 (bs, 1H), 6.98 (s, 1H), 5.35 (dd, 1H, J = 7.8, J = 2.2 Hz), 4.34–4.27 (m, 1H), 4.03–3.96 (m, 1H) ppm.

4.7.2.11. 1-(3,4-Dichlorophenyl)-2-(1H-imidazol-1-yl)ethanol (10d) [113,114]. Synthesized from 2-bromo-1-(3,4-dichlorophenyl)ethanone (**8d**) according to the general procedure to afford **10d** as a white solid in 75% yield, ^{1}H NMR (400 MHz, CDCl₃): δ 7.49–7.41 (m, 3H), 7.14 (dd, 1H, J = 8.3, J = 2.0 Hz), 7.01 (bs, 1H), 6.91 (s, 1H), 4.95 (m, 1H), 4.18–4.01 (m, 2H) ppm.

4.7.2.12. 1-(3-Chlorophenyl)-2-(1H-imidazol-1-yl)ethanol (10e) [113,114]. Synthesized from 2-bromo-1-(3-chlorophenyl)ethanone (**8e**) according to the general procedure to afford **10a** as a white solid in 77% yield, ^{1}H NMR (400 MHz, CDCl₃): δ 7.42 (bs, 1H), 7.38 (s, 1H), 7.34–7.28 (m, 2H), 7.22–7.16 (m, 1H), 6.99 (bs, 1H), 6.91 (s, 1H), 4.96–4.90 (m, 1H), 4.18–4.03 (m, 2H) ppm.

4.7.2.13. 1-(4-chlorophenyl)-2-(1H-imidazol-1-yl)ethanol (10f) [76]. Synthesized from 2-bromo-1-(4-chlorophenyl)ethanone (**8f**) according to the general procedure to afford **10f** as a white solid in 68% yield, ^{1}H NMR (400 MHz, CD₃OD): δ 7.50 (bs, 1H), 7.35–7.27 (m, 4H), 7.07 (bs, 1H), 6.90 (s, 1H), 4.95–4.90 (m, 1H), 4.26–4.12 (m, 2H) ppm.

4.7.2.14. 1-(2,6-Dichlorophenyl)-2-(1H-imidazol-1-yl)ethanol (10g) [113,114]. Synthesized from 2-bromo-1-(2,6-dichlorophenyl)

ethanone (**8g**) according to the general procedure to afford **10g** as a white solid in 65% yield, ^{1}H NMR (400 MHz, CD₃OD): δ 7.63 (bs, 1H), 7.41–7.36 (m, 2H), 7.29–7.23 (m, 1H), 7.08 (bs, 1H), 6.93 (s, 1H), 5.75–5.69 (m, 1H), 4.69–4.61 (m, 1H), 4.49–4.42 (m, 1H) ppm.

4.7.2.15. 2-(1-Hydroxy-2-(1H-imidazol-1-yl)ethyl)phenol (10h). Synthesized from 2-bromo-1-(2-hydroxyphenyl)ethanone (**8h**) according to the general procedure to afford **10h** as a white solid in 70% yield, m.p. 149–152 °C, IR (film): ν_{max}: 3360, 2938, 1594, 1511, 1454, 1282, 820, 752 cm^{-1}, ^{1}H NMR (400 MHz, CDCl₃): δ 7.42 (bs, 1H), 7.14 (td, 1H, J = 7.6, J = 1.5 Hz), 7.05–7.01 (m, 1H), 6.94 (bs, 1H), 6.90 (s, 1H), 6.84–6.77 (m, 2H), 5.03–4.97 (m, 1H), 4.23–4.11 (m, 2H) ppm. ^{13}C NMR (100 MHz, CD₃OD): δ 153.9, 137.5, 128.2, 127.2, 126.8, 126.3, 120.2, 119.2, 114.6, 68.7, 52.3 ppm. ESI-TOF-HRMS: m/z calcd for (M+H) $C_{11}H_{12}N_2O_2$ 205.0977 found 205.0984.

4.7.2.16. 1-(2,4-Dichlorophenyl)-2-(1H-1,2,4-triazol-1-yl)ethanol (10i) [115,116]. Synthesized from 2-bromo-1-(2,4-dichlorophenyl) ethanone (**8a**) and 1H-1,2,4-triazole according to the general procedure to afford **10i** as a white solid in 74% yield, ^{1}H NMR (400 MHz, CD₃OD): δ 8.43 (s, 1H), 7.96 (s, 1H), 7.56 (d, 1H, J = 8.2 Hz), 7.47 (d, 1H, J = 6.0 Hz) 7.36 (dd, 1H, J = 8.3, J = 2.1 Hz), 5.41–5.36 (m, 1H), 4.51–4.44 (m, 1H), 4.38–4.30 (m, 1H) ppm.

4.7.2.17. 1-(2,4-Dichlorophenyl)-2-(1H-1,2,3-triazol-5-yl)ethanol (13). Activated zinc powder (5.75 mmol, 1.15 eq) was placed in a flame-dried round-bottom flask (50 mL) fitted with a magnetic stir bar. 2,4-Dichlorobenzaldehyde (5 mmol, 1 eq) and propargyl-bromide (5.75 mmol, 1.15 eq) were added. The resulting mixture was vigorously stirred for 1 h at room temperature. After reaction completion, sat. aq. soln of NH_4Cl was poured into the mixture and stirred for several minutes. Diethyl ether was added and the organic layer was separated and dried over anhydrous $MgSO_4$. The residue was purified by flash chromatography on silica gel giving 1-phenylpropargylalcohol (**12**). To a stirred solution of **12** (1 mmol, 1 eq) and CuI (0.05 mmol, 0.05 eq) in DMF/MeOH solution (2 mL 9:1) under an argon atmosphere was added trimethylsilyl azide (1.5 mmol, 1.5 eq). The resulting solution was stirred at 100 °C for 10–12 h. After consumption of ethynyl substrate, the mixture was cooled to room temperature and the precipitate was filtered off and the solution concentrated under reduced pressure. The crude residue was purified by silica gel column chromatography to afford **13** as an oil in 60% yield. IR (film): ν_{max}: 3142, 2932, 2828, 1588, 1560, 1467, 1069, 1043, 818, 789 cm^{-1}, ^{1}H NMR (400 MHz, CD₃OD): δ 8.20 (s, 1H), 7.54–7.47 (m, 2H), 7.38–7.33 (m, 1H), 5.37–5.30 (m, 1H), 3.39–3.33 (m, 1H), 3.20–3.12 (m, 1H) ppm. ^{13}C NMR (100 MHz, CD₃OD): δ 140.5, 133.2, 132.1, 128.5, 128.4, 127.0, 68.5, 32.4 ppm. ESI-TOF-HRMS: m/z calcd for (M+H) $C_{10}H_9N_3Cl_2O$ 258.0201 found 258.0191.

4.7.2.18. 1-(2,4-Dichlorophenyl)-1H-imidazole (15) [79]. Synthesized from 2,4-dichloro-1-fluorobenze and 1-(trimethylsilyl)-1H-imidazole, according to reported procedure [79] to afford 15 as a solid in 70% yield. ^{1}H NMR (400 MHz, CDCl₃): δ 7.70 (s, 1H), 7.60 (d, 1H, J = 2.2 Hz), 7.40 (dd, 1H, J = 8.3, J = 2.2 Hz), 7.32 (d, 1H, J = 8.4 Hz), 7.25 (bs, 1H), 7.16 (bs, 1H) ppm.

Disclosure of potential conflict of interest

Acknowledgments

Appendix A. Supplementary data

Supplementary data associated with this article can be found in the online version, at http://dx.doi.org/10.1016/j.ejmech.2014.06.078. These data include MOL files and InChiKeys of the most important compounds described in this article.

References

[1] L. Vécsei, L. Szalárdy, F. Fülöp, J. Toldi, Kynurenines in the CNS: recent advances and new questions, Nat. Rev. Drug Dis. 12 (2013) 64–82, http://dx.doi.org/10.1038/nrd3793.

[2] H. Barth, S. Raghuraman, Persistent infectious diseases say − IDO. Role of indoleamine-2,3-dioxygenase in disease pathogenesis and implications for therapy, Crit. Rev. Microbiol. 40 (2014) 360–368, http://dx.doi.org/10.3109/1040841X.2012.742037.

[3] T.W. Stone, N. Stoy, L.G. Darlington, An expanding range of targets for kynurenine metabolites of tryptophan, Trends Pharmacol. Sci. 34 (2013) 136–143, http://dx.doi.org/10.1016/j.tips.2012.09.006.

[4] D.H. Munn, A.L. Mellor, Indoleamine 2,3 dioxygenase and metabolic control of immune responses, Trends Immunol. 34 (2013) 137–143, http://dx.doi.org/10.1016/j.it.2012.10.001.

[5] S. Yamamoto, O. Hayaishi, Tryptophan pyrrolase of rabbit intestine. D- and L-tryptophan-cleaving enzyme or enzymes, J. Biol. Chem. 242 (1967) 5260–5266.

[6] M. Platten, W. Wick, B.J. Van den Eynde, Tryptophan catabolism in cancer: beyond IDO and tryptophan depletion, Cancer Res. 72 (2012) 5435–5440, http://dx.doi.org/10.1158/0008-5472.CAN-12-0569.

[7] C. Uyttenhove, L. Pilotte, I. Théate, V. Stroobant, D. Colau, N. Parmentier, T. Boon, B.J. Van den Eynde, Evidence for a tumoral immune resistance mechanism based on tryptophan degradation by indoleamine 2,3-dioxygenase, Nat. Med. 9 (2003) 1269–1274, http://dx.doi.org/10.1038/nm934.

[8] C. Du, Y. Wang, The immunoregulatory mechanisms of carcinoma for its survival and development, J. Exp. Clin. Cancer Res. 30 (2011) 12, http://dx.doi.org/10.1186/1756-9966-30-12.

[9] C.A. Opitz, U.M. Litzenburger, F. Sahm, M. Ott, I. Tritschler, S. Trump, T. Schumacher, L. Jestaedt, D. Schrenk, M. Weller, M. Jugold, G.J. Guillemin, C.L. Miller, C. Lutz, B. Radlwimmer, I. Lehmann, A. von Deimling, W. Wick, M. Platten, An endogenous tumour-promoting ligand of the human aryl hydrocarbon receptor, Nature 478 (2011) 197–203, http://dx.doi.org/10.1038/nature10491.

[10] L. Pilotte, P. Larrieu, V. Stroobant, D. Colau, E. Dolušić, R. Frédérick, E.D. Plaen, C. Uyttenhove, J. Wouters, B. Masereel, B.J. Van den Eynde, Reversal of tumoral immune resistance by inhibition of tryptophan 2,3-dioxygenase, Proc. Natl. Acad. Sci. U. S. A. 109 (2012) 2497–2502, http://dx.doi.org/10.1073/pnas.1113873109.

[11] J. Godin-Ethier, L.-A. Hanafi, C.A. Piccirillo, R. Lapointe, Indoleamine 2,3-dioxygenase expression in human cancers: clinical and immunologic perspectives, Clin. Canc. Res. 17 (2011) 6985–6991, http://dx.doi.org/10.1158/1078-0432.CCR-11-1331.

[12] J.B. Katz, A.J. Muller, G.C. Prendergast, Indoleamine 2,3-dioxygenase in T-cell tolerance and tumoral immune escape, Immunol. Rev. 222 (2008) 206–221, http://dx.doi.org/10.1111/j.1600-065X.2008.00610.x.

[13] G.C. Prendergast, Immune escape as a fundamental trait of cancer: focus on IDO, Oncogene 27 (2008) 3889–3900, http://dx.doi.org/10.1038/onc.2008.35.

[14] A.J. Muller, J.B. DuHadaway, P.S. Donover, E. Sutanto-Ward, G.C. Prendergast, Inhibition of indoleamine 2,3-dioxygenase, an immunoregulatory target of the cancer suppression gene bin1, potentiates cancer chemotherapy, Nat. Med. 11 (2005) 312–319, http://dx.doi.org/10.1038/nm1196.

[15] X. Liu, N. Shin, H.K. Koblish, G. Yang, Q. Wang, K. Wang, L. Leffet, M.J. Hansbury, B. Thomas, M. Rupar, P. Waeltz, K.J. Bowman, P. Polam, R.B. Sparks, E.W. Yue, Y. Li, R. Wynn, J.S. Fridman, T.C. Burn, A.P. Combs, R.C. Newton, P.A. Scherle, Selective inhibition of IDO1 effectively regulates mediators of antitumor immunity, Blood 115 (2010) 3520–3530, http://dx.doi.org/10.1182/blood-2009-09-246124.

[16] E. Dolušić, R. Frédérick, Indoleamine 2,3-dioxygenase inhibitors: a patent review (2008–2012), Expert Opin. Ther. Targets 23 (2013) 1367–1381, http://dx.doi.org/10.1517/13543776.2013.827662.

[17] E.W. Yue, B. Douty, B. Wayland, M. Bower, X. Liu, L. Leffet, Q. Wang, K.J. Bowman, M.J. Hansbury, C. Liu, M. Wei, Y. Li, R. Wynn, T.C. Burn, H.K. Koblish, J.S. Fridman, B. Metcalf, P.A. Scherle, A.P. Combs, Discovery of potent competitive inhibitors of indoleamine 2,3-dioxygenase with in vivo pharmacodynamic activity and efficacy in a mouse melanoma model, J. Med. Chem. 52 (2009) 7364–7367, http://dx.doi.org/10.1021/jm900518f.

[18] H.K. Koblish, M.J. Hansbury, K.J. Bowman, G. Yang, C.L. Neilan, P.J. Haley, T.C. Burn, P. Waeltz, R.B. Sparks, E.W. Yue, A.P. Combs, P.A. Scherle, K. Vaddi, J.S. Fridman, Hydroxyamidine inhibitors of indoleamine-2,3-dioxygenase potently suppress systemic tryptophan catabolism and the growth of ido-expressing tumors, Mol. Cancer Ther. 9 (2010) 489–498, http://dx.doi.org/10.1158/1535-7163.MCT-09-0628.

[19] M.R. Mautino, F.A. Jaipuri, J. Waldo, S. Kumar, J. Adams, C. Van Allen, A. Marcinowicz-Flick, D. Munn, N.N. Vahanian, C.J. Link, NLG919, a novel indoleamine-2,3-dioxygenase (IDO)-pathway inhibitor drug candidate for cancer therapy [abstract]Proceedings of the 104th Annual Meeting of the American Association for Cancer Research; 2013 Apr 6–10; Washington, DC, Cancer Res. vol. 73 (2013). Philadelphia (PA).

[20] N. Thorne, D.S. Auld, J. Inglese, Apparent activity in high-throughput screening: origins of compound-dependent assay interference, Curr. Opin. Chem. Biol. 14 (2010) 315–324, http://dx.doi.org/10.1016/j.cbpa.2010.03.020.

[21] E. Vottero, A. Balgi, K. Woods, S. Tugendreich, T. Melese, R.J. Andersen, A.G. Mauk, M. Roberge, Inhibitors of human indoleamine 2,3-dioxygenase identified with a target-based screen in yeast, Biotechnol. J. 1 (2006) 282–288, http://dx.doi.org/10.1002/biot.200600001.

[22] M. Cerejo, G. Andrade, C. Roca, J. Sousa, C. Rodrigues, R. Pinheiro, S. Chatterjee, H. Vieira, P. Calado, A powerful yeast-based screening assay for the identification of inhibitors of indoleamine 2,3-dioxygenase, J. Biomol. Screen. 17 (2012) 1362–1371, http://dx.doi.org/10.1177/1087057112452595.

[23] D. Meininger, L. Zalameda, Y. Liu, L.P. Stepan, L. Borges, J.D. McCarter, C.L. Sutherland, Purification and kinetic characterization of human indoleamine 2,3-dioxygenases 1 and 2 (IDO1 and IDO2) and discovery of selective IDO1 inhibitors, Biochim. Biophys. Acta 1814 (2011) 1947–1954, http://dx.doi.org/10.1016/j.bbapap.2011.07.023.

[24] P. Tomek, B.D. Palmer, J.U. Flanagan, S.-P.S. Fung, D.J.A. Bridewell, J.F. Jamie, L.-M. Ching, Formation of an N-formylkynurenine-derived fluorophore and its use for measuring indoleamine 2,3-dioxygenase 1 activity, Anal. Bioanal. Chem. 405 (2013) 2515–2524, http://dx.doi.org/10.1007/s00216-012-6650-y.

[25] S.-P.S. Fung, H. Wang, P. Tomek, C.J. Squire, J.U. Flanagan, B.D. Palmer, D.J. Bridewell, S.M. Tijono, J.F. Jamie, L.-M. Ching, Discovery and characterisation of hydrazines as inhibitors of the immune suppressive enzyme, indoleamine 2,3-dioxygenase 1 (IDO1), Bioorg. Med. Chem. 21 (2013) 7595–7603, http://dx.doi.org/10.1016/j.bmc.2013.10.037.

[26] S.M. Bakmiwewa, A. Fatokun, A. Tran, R.J. Payne, N.H. Hunt, H.J. Ball, Identification of selective inhibitors of indoleamine 2,3-dioxygenase 2, Bioorg. Med. Chem. Lett. 22 (2012) 7641–7646, http://dx.doi.org/10.1016/j.bmcl.2012.10.010.

[27] A. Mullard, Drug repurposing programmes get lift off, Nat. Rev. Drug Dis. 11 (2012) 505–506, http://dx.doi.org/10.1038/nrd3776.

[28] J. Seidler, S.L. McGovern, T.N. Doman, B.K. Shoichet, Identification and prediction of promiscuous aggregating inhibitors among known drugs, J. Med. Chem. 46 (2003) 4477–4486, http://dx.doi.org/10.1021/jm030191r.

[29] K.M. Soares, N. Blackmon, T.Y. Shun, S.N. Shinde, H.K. Takyi, P. Wipf, J.S. Lazo, P.A. Johnston, Profiling the NIH Small Molecule Repository for compounds that generate H_2O_2 by redox cycling in reducing environments, Assay Drug Dev. Technol. 8 (2010) 152–174, http://dx.doi.org/10.1089/adt.2009.0247.

[30] M. Hann, B. Hudson, X. Lewell, R. Lifely, L. Miller, N. Ramsden, Strategic pooling of compounds for high-throughput screening, J. Chem. Inf. Comput. Sci. 39 (1999) 897–902, http://dx.doi.org/10.1021/ci990423o.

[31] J.F. Blake, Identification and evaluation of molecular properties related to preclinical optimization and clinical fate, Med. Chem. 1 (2005) 649–655, http://dx.doi.org/10.2174/15734060577459808.

[32] J.R. Huth, R. Mendoza, E.T. Olejniczak, R.W. Johnson, D.A. Cothron, Y. Liu, C.G. Lerner, J. Chen, P.J. Hajduk, ALARM NMR: a rapid and robust experimental method to detect reactive false positives in biochemical screens, J. Am. Chem. Soc. 127 (2005) 217–224, http://dx.doi.org/10.1021/ja0455547.

[33] J.B. Baell, G. Holloway, New substructure filters for removal of pan assay interference compounds (PAINS) from screening libraries and for their exclusion in bioassays, J. Med. Chem. 53 (2010) 2719–2740, http://dx.doi.org/10.1021/jm901137j.

[34] R.F. Bruns, I. Watson, Rules for identifying potentially reactive or promiscuous compounds, J. Med. Chem. 55 (2012) 9763–9772, http://dx.doi.org/10.1021/jm301008n.

[35] J.T. Pearson, S. Siu, D.P. Meininger, L.C. Wienkers, D.A. Rock, In vitro modulation of cytochrome p450 reductase supported indoleamine 2,3-dioxygenase activity by allosteric effectors cytochrome b(5) and methylene blue, Biochemistry 49 (2010) 2647–2656, http://dx.doi.org/10.1021/bi100022c.

[36] L. Lor, J. Schneck, D.E. McNulty, E. Diaz, M. Brandt, S.H. Thrall, B. Schwartz, A simple assay for detection of small-molecule redox activity, J. Biomol. Screen. 12 (2007) 881–890, http://dx.doi.org/10.1177/1087057107304113.

[37] P. Johnston, Redox cycling compounds generate H_2O_2 in HTS buffers containing strong reducing reagents—real hits or promiscuous artifacts? Curr. Opin. Chem. Biol. 15 (2011) 174–182, http://dx.doi.org/10.1016/j.cbpa.2010.10.022.

[38] B.K. Shoichet, Screening in a spirit haunted world, Drug Discov. Today 11 (2006) 607–615, http://dx.doi.org/10.1016/j.drudis.2006.05.014.

[39] B.Y. Feng, B.K. Shoichet, A detergent-based assay for the detection of promiscuous inhibitors, Nat. Protoc. 1 (2006) 550–553, http://dx.doi.org/10.1038/nprot.2006.77.

[40] U.F. Röhrig, L. Awad, A. Grosdidier, P. Larrieu, V. Stroobant, D. Colau, V. Cerundolo, A.J.G. Simpson, P. Vogel, B.J. Van den Eynde, V. Zoete, O. Michielin, Rational design of indoleamine 2,3-dioxygenase inhibitors, J. Med. Chem. 53 (2010) 1172–1189, http://dx.doi.org/10.1021/jm9014718.

[41] U.F. Röhrig, S.R. Majjigapu, A. Grosdidier, S. Bron, V. Stroobant, L. Pilotte, D. Colau, P. Vogel, B.J. Van den Eynde, V. Zoete, O. Michielin, Rational design of 4-aryl-1,2,3-triazoles for indoleamine 2,3-dioxygenase 1 inhibition, J. Med. Chem. 55 (2012) 5270–5290, http://dx.doi.org/10.1021/jm300260v.

[42] T. Ohnishi, F. Hirata, O. Hayaishi, Indoleamine 2,3-dioxygenase. Potassium superoxide as substrate, J. Biol. Chem. 252 (1977) 4643–4647.

[43] J.-H. Zhang, A simple statistical parameter for use in evaluation and validation of high throughput screening assays, J. Biomol. Screen. 4 (1999) 67–73, http://dx.doi.org/10.1177/108705719900400206.

[44] Y. Eberhard, S.P. McDermott, X. Wang, M. Gronda, A. Venugopal, T.E. Wood, R. Hurren, A. Datti, R. a. Batey, J. Wrana, W.E. Antholine, J.E. Dick, J. Dick, A.D. Schimmer, Chelation of intracellular iron with the antifungal agent ciclopirox olamine induces cell death in leukemia and myeloma cells, Blood 114 (2009) 3064–3073, http://dx.doi.org/10.1182/blood-2009-03-209965.

[45] M.O. Griffin, E. Fricovsky, G. Ceballos, F. Villarreal, Tetracyclines: a pleitropic family of compounds with promising therapeutic properties. Review of the literature, Am. J. Physiol. Cell P. H. 299 (2010) C539–C548, http://dx.doi.org/10.1152/ajpcell.00047.2010.

[46] N. Strushkevich, S. Usanov, H.-W. Park, Structural basis of human CYP51 inhibition by antifungal azoles, J. Mol. Biol. 397 (2010) 1067–1078, http://dx.doi.org/10.1016/j.jmb.2010.01.075.

[47] S.F. Muakkassah, W.C. Yang, Mechanism of the inhibitory action of phenelzine on microsomal drug metabolism, J. Pharmacol. Exp. Ther. 219 (1981) 147–155.

[48] C.J.D. Austin, F. Astelbauer, P. Kosim-Satyaputra, H.J. Ball, R.D. Willows, J.F. Jamie, N.H. Hunt, Mouse and human indoleamine 2,3-dioxygenase display some distinct biochemical and structural properties, Amino Acids 36 (2009) 99–106, http://dx.doi.org/10.1007/s00726-008-0037-6.

[49] A.C. Terentis, M. Freewan, T.S.S. Plaza, M.J. Raftery, R. Stocker, S.R. Thomas, The selenazal drug ebselen potently inhibits indoleamine 2,3-dioxygenase by targeting enzyme cysteine residues, Biochemistry 49 (2010) 591–600, http://dx.doi.org/10.1021/bi901546e.

[50] B. Shoichet, A. Doak, K. Ziebart, Aggregator Advisor, 2013. http://advisor.bkslab.org.

[51] A.J. Ryan, N.M. Gray, P.N. Lowe, C.-w. Chung, Effect of detergent on "promiscuous" inhibitors, J. Med. Chem. 46 (2003) 3448–3451, http://dx.doi.org/10.1021/jm0340896.

[52] H.C. Brastianos, E. Vottero, B.O. Patrick, R.V. Soest, T. Matainaho, A.G. Mauk, R.J. Andersen, Exiguamine a, an indoleamine-2,3-dioxygenase (IDO) inhibitor isolated from the marine sponge neopetrosia exigua, J. Am. Chem. Soc. 128 (2006) 16046–16047, http://dx.doi.org/10.1021/ja067211.

[53] R. Andersen, A. Pereira, X.-H. Huang, G. Mauk, E. Vottero, M. Roberge, A. Balgi. Indoleamine 2,3-Dioxygenase (IDO) Inhibitors. Patent WO 2006/005185 (01 2006).

[54] A. Pereira, E. Vottero, M. Roberge, A.G. Mauk, R.J. Andersen, Indoleamine 2,3-dioxygenase inhibitors from the northeastern pacific marine hydroid garveia annulata, J. Nat. Prod. 69 (2006) 1496–1499, http://dx.doi.org/10.1021/np060111x.

[55] R. Andersen, M. Leblanc, H. Brastianos, E. Vottero, M. Roberge, G. Mauk, G. Carr. Substituted Quinone Indoleamine 2,3-Dioxygenase (IDO) Inhibitors and Synthesis and Uses Thereof. Patent WO 2008/052352 (05 2008).

[56] G. Carr, M.K.W. Chung, A.G. Mauk, R.J. Andersen, Synthesis of indoleamine 2,3-dioxygenase inhibitory analogues of the sponge alkaloid exiguamine a, J. Med. Chem. 51 (2008) 2634–2637, http://dx.doi.org/10.1021/jm800143h.

[57] S. Kumar, W. Malachowski, J. Duhadaway, J. Lalonde, P. Carroll, D. Jaller, R. Metz, G. Prendergast, A. Muller, Indoleamine 2,3-dioxygenase is the anticancer target for a novel series of potent naphthoquinone-based inhibitors, J. Med. Chem. 51 (2008) 1706–1718, http://dx.doi.org/10.1021/jm7014155.

[58] G. Carr, W. Tay, H. Bottriell, S.K. Andersen, A.G. Mauk, R.J. Andersen, Plectosphaeroic acids a, b, and c, indoleamine 2,3-dioxygenase inhibitors produced in culture by a marine isolate of the fungus Plectosphaerella cucumerina, Org. Lett. 11 (2009) 2996–2999, http://dx.doi.org/10.1021/ol900972j.

[59] E. Dolušić, P. Larrieu, C. Meinguet, D. Colette, A. Rives, S. Blanc, T. Ferain, L. Pilotte, V. Stroobant, J. Wouters, B. Van den Eynde, B. Masereel, E. Delfourne, R. Frédérick, Indoleamine 2,3-dioxygenase inhibitory activity of derivatives of marine alkaloid tsitsikammamine A, Bioorg. Med. Chem. Lett. 23 (2013) 47–54, http://dx.doi.org/10.1016/j.bmcl.2012.11.036.

[60] D.J. Bridewell, J. Sperry, J.R. Smith, P. Kosim-Satyaputra, L.-M. Ching, J.F. Jamie, M. Brimble, Natural product-inspired pyranonaphthoquinone inhibitors of indoleamine 2,3-dioxygenase-1 (IDO-1), Aust. J. Chem. 66 (2013) 40, http://dx.doi.org/10.1071/CH12393.

[61] R. Pasceri, D. Siegel, D. Ross, C.J. Moody, Aminophenoxazinones as inhibitors of indoleamine 2,3-dioxygenase (IDO). Synthesis of exfoliazone and chandrananimycin A, J. Med. Chem. 56 (2013) 3310–3317, http://dx.doi.org/10.1021/jm400049z.

[62] H.E. Flick, J.M. Lalonde, W.P. Malachowski, A.J. Muller, The tumor-selective cytotoxic agent β-lapachone is a potent inhibitor of IDO1, Int. J. Tryptophan Res. 6 (2013) 35–45, http://dx.doi.org/10.4137/IJTR.S12094.

[63] G. Pantouris, C.G. Mowat, Antitumour agents as inhibitors of tryptophan 2,3-dioxygenase, Biochem. Biophys. Res. Commun. 443 (2014) 28–31, http://dx.doi.org/10.1016/j.bbrc.2013.11.037.

[64] P. Rana, R. Naven, A. Narayanan, Y. Will, L.H. Jones, Chemical motifs that redox cycle and their associated toxicity, MedChemComm 4 (2013) 1175, http://dx.doi.org/10.1039/c3md00149k.

[65] S. Bittner, When quinones meet amino acids: chemical, physical and biological consequences, Amino acids 30 (2006) 205–224, http://dx.doi.org/10.1007/s00726-005-0298-2.

[66] S. Kumar, D. Jaller, B. Patel, J.M. LaLonde, J.B. DuHadaway, W.P. Malachowski, G.C. Prendergast, A.J. Muller, Structure based development of phenylimidazole-derived inhibitors of indoleamine 2,3-dioxygenase, J. Med. Chem. 51 (2008) 4968–4977, http://dx.doi.org/10.1021/jm800512z.

[67] M. Mautino, S. Kumar, F. Jaipuri, J. Waldo, T. Kesharwani, N. N. Vahanian, C. J. Link, J. Lalonde, G. Prendergast, A. Muller, W. Malachowski. IDO Inhibitors. Patent WO 2009/132238.

[68] M. Mautino, S. Kumar, F. Jaipuri, J. Waldo, T. Kesharwani, X. Zhang. Imidazole Derivatives as IDO Inhibitors. Patent WO 2011/056652.

[69] M. Mautino, S. Kumar, J. Waldo, F. Jaipuri, T. Kesharwani, X. Zhang. Fused Imidazole Derivatives Useful as IDO Inhibitors. Patent WO 2012/142237.

[70] H. Sugimoto, S. Oda, T. Otsuki, T. Hino, T. Yoshida, Y. Shiro, Crystal structure of human indoleamine 2,3-dioxygenase: catalytic mechanism of O_2 incorporation by a heme-containing dioxygenase, Proc. Natl. Acad. Sci. U. S. A. 103 (2006) 2611–2616, http://dx.doi.org/10.1073/pnas.0508996103.

[71] E. Dolušić, P. Larrieu, S. Blanc, F. Sapunaric, J. Pouyez, L. Moineaux, D. Colette, V. Stroobant, L. Pilotte, D. Colau, T. Ferain, G. Fraser, M. Galleni, J.-M. Frère, B. Masereel, B. Van den Eynde, J. Wouters, R. Frédérick, Discovery and preliminary SARS of keto-indoles as novel indoleamine 2,3-dioxygenase (IDO) inhibitors, Eur. J. Med. Chem. 46 (2011) 3058–3065, http://dx.doi.org/10.1016/j.ejmech.2011.02.049.

[72] J.R. Smith, K.J. Evans, A. Wright, R.D. Willows, J.F. Jamie, R. Griffith, Novel indoleamine 2,3-dioxygenase-1 inhibitors from a multistep in silico screen, Bioorg. Med. Chem. 20 (2012) 1354–1363, http://dx.doi.org/10.1016/j.bmc.2011.10.068.

[73] A. Grosdidier, V. Zoete, O. Michielin, Fast docking using the charmm force field with eadock dss, J. Comput. Chem. 32 (2011) 2149–2159, http://dx.doi.org/10.1002/jcc.21797.

[74] E. Cuevas Yañez, A. Canul Sánchez, J.M. Serrano Becerra, J.M. Muchowski, R. Cruz Almanza, Synthesis of miconazole and Analogs through a Carbenoid Intermediate, Rev. Soc. Quim. Mex. 48 (2004) 49–52.

[75] J.Z. Vlahakis, C. Lazar, G. Roman, D. Vukomanovic, K. Nakatsu, W.A. Szarek, Heme oxygenase inhibition by α-(1H-imidazol-1-yl)-ω-phenylalkanes: effect of introduction of heteroatoms in the alkyl linker, ChemMedChem 7 (2012) 897–902, http://dx.doi.org/10.1002/cmdc.201100602.

[76] G. Roman, J.Z. Vlahakis, D. Vukomanovic, K. Nakatsu, W.A. Szarek, Heme oxygenase inhibition by 1-aryl-2-(1h-imidazol-1-yl/1h-1,2,4-triazol-1-yl) ethanones and their derivatives, ChemMedChem 5 (2010) 1541–1555, http://dx.doi.org/10.1002/cmdc.201000120.

[77] J.-X. Wang, X. Jia, T. Meng, L. Xin, Rapid and solvent-free synthesis of Homoallyl or Homopropargyl alcohols mediated by zinc powder, Synthesis 2005 (2005) 2838–2844, http://dx.doi.org/10.1055/s-2005-872178.

[78] T. Jin, S. Kamijo, Y. Yamamoto, Copper-catalyzed synthesis of N-unsubstituted 1,2,3-triazoles from nonactivated terminal alkynes, Eur. J. Org. Chem. 18 (2004) 3789–3791, http://dx.doi.org/10.1002/ejoc.200400442.

[79] D. Dehe, I. Munstein, A. Reis, W.R. Thiel, Mild transition-metal-free amination of fluoroarenes catalyzed by fluoride ions, J. Org. Chem. 76 (2011) 1151–1154, http://dx.doi.org/10.1021/jo102063s.

[80] K. Matsuno, K. Takai, Y. Isaka, Y. Unno, M. Sato, O. Takikawa, A. Asai, S-benzylisothiourea derivatives as small-molecule inhibitors of indoleamine-2,3-dioxygenase, Bioorg. Med. Chem. Lett. 20 (2010) 5126–5129, http://dx.doi.org/10.1016/j.bmcl.2010.07.025.

[81] A. Grosdidier, V. Zoete, O. Michielin, EADock: docking of small molecules into protein active sites with a multiobjective evolutionary optimization, Proteins 67 (2007) 1010–1025, http://dx.doi.org/10.1002/prot.21367.

[82] A. Grosdidier, V. Zoete, O. Michielin, Blind docking of 260 protein-ligand complexes with EADock 2.0, J. Comput. Chem. 30 (2009) 2021–2030, http://dx.doi.org/10.1002/jcc.21202.

[83] V. Zoete, A. Grosdidier, M. Cuendet, O. Michielin, Use of the FACTS solvation model for protein-ligand docking calculations. Application to EADock, J. Mol. Recognit. 23 (2010) 457–461, http://dx.doi.org/10.1002/jmr.1012.

[84] V. Zoete, A. Grosdidier, T. Schuepbach, O. Michielin, Attracting Cavities (manuscript in preparation).

[85] A.D. MacKerell Jr., D. Bashford, M. Bellott, R.L. Dunbrack Jr., J.D. Evanseck, M.J. Field, S. Fischer, J. Gao, H. Guo, S. Ha, D. Joseph-McCarthy, L. Kuchnir, K. Juczera, F.T.K. Lau, C. Mattos, S. Michnik, T. Ngo, D.T. Nguyen, B. Prodhom, W.E. Reiher III, B. Roux, M. Schlenkrich, J.C. Smith, R. Stote, J. Straub, M. Watanabe, J. Wiórkiewicz-Kuczera, D. Yin, M. Karplus, All-atom empirical potential for molecular modeling and dynamics studies of proteins, J. Phys. Chem. B 102 (1998) 3586–3616, http://dx.doi.org/10.1021/jp973084f.

[86] U. Haberthür, A. Caflisch, Facts: fast analytical continuum treatment of solvation, J. Comput. Chem. 29 (2008) 701–715, http://dx.doi.org/10.1002/jcc.20832.

[87] V. Zoete, A. Grosdidier, M. Cuendet, O. Michielin, Use of the FACTS solvation model for protein-ligand docking calculations. Application to EADock, J. Mol. Recognit. 23 (2010) 457–461, http://dx.doi.org/10.1002/jmr.1012.

[88] V. Zoete, M.A. Cuendet, A. Grosdidier, O. Michielin, SwissParam: a fast force field generation tool for small organic molecules, J. Comput. Chem. 32 (2011) 2359–2368, http://dx.doi.org/10.1002/jcc.21816.

[89] U.F. Röhrig, A. Grosdidier, V. Zoete, O. Michielin, Docking to heme proteins, J. Comput. Chem. 30 (2009) 2305–2315, http://dx.doi.org/10.1002/jcc.21244.

[90] B. Hess, C. Kutzner, D. van der Spoel, E. Lindahl, GROMACS 4: algorithms for highly efficient, load-balanced, and scalable molecular simulation, J. Chem. Theory Comput. 4 (2008) 435–447, http://dx.doi.org/10.1021/ct700301q.

[91] A.D. MacKerell, M. Feig, C.L. Brooks, Extending the treatment of backbone energetics in protein force fields: limitations of gas-phase quantum mechanics in reproducing protein conformational distributions in molecular dynamics simulations, J. Comput. Chem. 25 (2004) 1400–1415, http://dx.doi.org/10.1002/jcc.20065.

[92] P. Bjelkmar, P. Larsson, M.A. Cuendet, B. Hess, E. Lindahl, Implementation of the CHARMM force field in GROMACS: analysis of protein stability effects from correction maps, virtual interaction sites, and water models, J. Chem. Theory Comput. 6 (2010) 459–466, http://dx.doi.org/10.1021/ct900549r.

[93] W.L. Jorgensen, J. Chandrasekhar, J.D. Madura, R.W. Impey, M.L. Klein, Comparison of simple potential functions for simulating liquid water, J. Chem. Phys. 79 (1983) 926, http://dx.doi.org/10.1063/1.445869.

[94] U. Essmann, L. Perera, M.L. Berkowitz, T. Darden, H. Lee, L.G. Pedersen, A smooth particle mesh Ewald method, J. Chem. Phys. 103 (1995) 8577, http://dx.doi.org/10.1063/1.470117.

[95] B. Hess, P-LINCS: a parallel linear constraint solver for molecular simulation, J. Chem. Theory Comput. 4 (2008) 116–122, http://dx.doi.org/10.1021/ct700200b.

[96] G. Bussi, D. Donadio, M. Parrinello, Canonical sampling through velocity rescaling, J. Chem. Phys. 126 (2007) 014101, http://dx.doi.org/10.1063/1.2408420.

[97] H.J.C. Berendsen, J.P.M. Postma, W.F. van Gunsteren, A. DiNola, J.R. Haak, Molecular dynamics with coupling to an external bath, J. Chem. Phys. 81 (1984) 3684, http://dx.doi.org/10.1063/1.448118.

[98] M.J.S. Dewar, E.G. Zoebisch, E.F. Healy, J.J.P. Stewart, AM1: a new general purpose quantum mechanical molecular model, J. Am. Chem. Soc. 107 (1985) 3902–3909, http://dx.doi.org/10.1021/ja00299a024.

[99] M.J. Frisch, G.W. Trucks, H.B. Schlegel, G.E. Scuseria, M.A. Robb, J.R. Cheeseman, G. Scalmani, V. Barone, B. Mennucci, G.A. Petersson, H. Nakatsuji, M. Caricato, X. Li, H.P. Hratchian, A.F. Izmaylov, J. Bloino, G. Zheng, J.L. Sonnenberg, M. Hada, M. Ehara, K. Toyota, R. Fukuda, J. Hasegawa, M. Ishida, T. Nakajima, Y. Honda, O. Kitao, H. Nakai, T. Vreven, J.A. Montgomery Jr., J.E. Peralta, F. Ogliaro, M. Bearpark, J.J. Heyd, E. Brothers, K.N. Kudin, V.N. Staroverov, R. Kobayashi, J. Normand, K. Raghavachari, A. Rendell, J.C. Burant, S.S. Iyengar, J. Tomasi, M. Cossi, N. Rega, J.M. Millam, M. Klene, J.E. Knox, J.B. Cross, V. Bakken, C. Adamo, J. Jaramillo, R. Gomperts, R.E. Stratmann, O. Yazyev, A.J. Austin, R. Cammi, C. Pomelli, J.W. Ochterski, R.L. Martin, K. Morokuma, V.G. Zakrzewski, G.A. Voth, P. Salvador, J.J. Dannenberg, S. Dapprich, A.D. Daniels, Ö. Farkas, J.B. Foresman, J.V. Ortiz, J. Cioslowski, D.J. Fox, Gaussian 09 Revision A.1, Gaussian Inc, Wallingford CT, 2009.

[100] R.V. Bensasson, S. Sowlati-Hashjin, V. Zoete, D. Dauzonne, C.F. Matta, Physicochemical properties of exogenous molecules correlated with their biological efficacy as protectors against carcinogenesis and inflammation, Int. Rev. Phys. Chem. 32 (2013) 393–434, http://dx.doi.org/10.1080/0144235X.2013.767669.

[101] V. Barone, M. Cossi, Quantum calculation of molecular energies and energy gradients in solution by a conductor solvent model, J. Phys. Chem. A 102 (1998) 1995, http://dx.doi.org/10.1021/jp9716997.

[102] M. Cossi, N. Rega, G. Scalmani, V. Barone, Energies, structures, and electronic properties of molecules in solution with the C-PCM solvation model, J. Comput. Chem. 24 (2003) 669, http://dx.doi.org/10.1002/jcc.10189.

[103] E.J. Lynch, A.L. Speelman, B.A. Curry, C.S. Murillo, J.G. Gillmore, Expanding and testing a computational method for predicting the ground state reduction potentials of organic molecules on the basis of empirical correlation to experiment, J. Org. Chem. 77 (2012) 6423–6430, http://dx.doi.org/10.1021/jo300853k.

[104] A. Becke, Density-functional thermochemistry. iii. The role of exact exchange, J. Chem. Phys. 98 (1993) 5648–5652, http://dx.doi.org/10.1063/1.464913.

[105] C. Lee, W. Yang, R. Parr, Development of the Colle-Salvetti correlation-energy formula into a functional of the electron density, Phys. Rev. B 37 (1988) 785–789, http://dx.doi.org/10.1103/PhysRevB.37.785.

[106] D.D. Méndez-Hernández, P. Tarakeshwar, D. Gust, T. a. Moore, A.L. Moore, V. Mujica, Simple and accurate correlation of experimental redox potentials and DFT-calculated HOMO/LUMO energies of polycyclic aromatic hydrocarbons, J. Mol. Model 19 (2013) 2845–2848, http://dx.doi.org/10.1007/s00894-012-1694-7.

[107] W.N. Cannon, C.E. Powell, R.G. Jones, Studies of imidazoles. VII. Substituted 1-phenethylimidazoles and related compounds, J. Org. Chem. 22 (1957) 1323–1326, http://dx.doi.org/10.1021/jo01362a008.

[108] M.R. Cuberes, M. Moreno-Mañas, A. Trius, α-Lithiation of N-arylmethylimidazoles and triazoles: a general method for the synthesis of 1,2-diaryl-1-(N-azolyl)-ethanes, Synthesis 1985 (1985) 302–304, http://dx.doi.org/10.1055/s-1985-31187.

[109] Y. Wahbi, C. Tournaire, R. Caujolle, M. Payard, M. Linas, J. Seguela, Aliphatic ethers and esters of 1-(2,4-dichlorophenyl)-2-(1H-imidazolyl) ethanol: study of antifungal activity against yeasts and hydrophobic character, Eur. J. Med. Chem. 29 (1994) 701–706, http://dx.doi.org/10.1016/0223-5234(94)90032-9.

[110] G.M. Dulcevscaia, V.C. Kravtsov, F.Z. Macaev, G.G. Duca, E.P. Stingachi, S.I. Pogrebnoi, V.V. Boldescu, S.F. Clapco, J.P. Tiurina, A.A. Deseatnic-Ciloci, J. Lipkowski, S.-X. Liu, S. Decurtins, S.G. Baca, New copper(II) complexes with isoconazole: synthesis, structures and biological properties, Polyhedron 52 (2013) 106–114, http://dx.doi.org/10.1016/j.poly.2012.10.040.

[111] R. Torregrosa, I.M. Pastor, M. Yus, Solvent-free direct regioselective ring opening of epoxides with imidazoles, Tetrahedron 63 (2007) 469–473, http://dx.doi.org/10.1016/j.tet.2006.10.055.

[112] Y. Iwasaki, T. Fujita, H. Yabe, H. Hirao, K. Kitagawa, S. Futaki, T. Inoue, T. Matsuzaki, T. Akita, Synthesis and antifungal activity of a series of novel 2-propen-1-one, Yakugaku Zasshi 108 (1988) 942–950.

[113] G. Sharma-Singh, D.A. Brown, F.S. Pullen, A.G. Wright, Open access capillary electrophoresis. A walk up capillary electrophoresis service for the synthetic chemist, J. Chromatogr. A 888 (2000) 219–227.

[114] E. F. Godefroi, J. Heeres. 1-(Beta-aryl)Ethyl-Imidazole Derivatives. Patent DE 1940388 (1970).

[115] Z.-F. Li, F.-Y. Luo, Jingxi Huagong 22 (2005) 619–624.

[116] K. Oh, K. Nakai, K. Yamada, Y. Yoshizawa, Synthesis of novel triazole derivatives as potent inhibitor of allene oxide synthase (CYP74A), a key enzyme in jasmonic acid biosynthesis, J. Pestic. Sci. 37 (2012) 80–84, http://dx.doi.org/10.1584/jpestics.D11-006.

[117] E.F. Pettersen, T. Goddard, C. Huang, G. Couch, D. Greenblatt, E. Meng, T.E. Ferrin, UCSF Chimera — a visualization system for exploratory research and analysis, J. Comput. Chem. 25 (2004) 1605–1612, http://dx.doi.org/10.1002/jcc.20084.